This article has been accepted for publication in IEEE Transactions on Wireless Communications. This is the author's version which has not been fully edited and content may change prior to final publication. Citation information: DOI 10.1109/TWC.2025.3536615

Stochastic Differential Equations for Performance Analysis of Wireless Communication Systems

Eya Ben Amar, Nadhir Ben Rached, Raúl Tempone, and Mohamed-Slim Alouini, *Fellow, IEEE*

***Abstract*—This paper focuses on the performance analysis of time-varying fading channels, introducing a new general metric called fade duration. Fade duration measures the time during which a signal remains below a specified threshold within a fixed time interval. To model the signal, we utilize established models for the inphase and quadrature components, employing stochastic differential equations (SDEs) to capture the continuous-time statistical properties of the fading channel. We estimate the complementary cumulative distribution function (CCDF) of the fade duration in different fading environments using Monte Carlo simulations and analyze how various system parameters impact its behavior. To enhance the efficiency of our estimates, we leverage importance sampling (IS), a well-known variance-reduction technique, for accurately estimating the tail of the CCDF. The proposed IS scheme involves solving a high-dimensional controlled partial differential equation. To overcome the curse of dimensionality, we use Markovian projection to develop a novel one-dimensional SDE for signal envelope variations, enhancing the computational feasibility of IS. We present numerical results for the CCDF of fade duration in Rayleigh and Rice environments using our proposed IS estimators.**

***Index Terms*—Fade duration, fading channels, importance sampling, Markovian projection, Monte Carlo, stochastic differential equations.**

I. Introduction

The performance analysis of wireless communication systems plays a critical role in understanding, evaluating, and optimizing their behavior under various conditions and constraints. Recent works have focused on assessing and modeling the performance of various types of wireless systems [1]–[6]. When we consider the temporal dynamics of the signal, this analysis becomes increasingly challenging.

Outage probability is the most commonly known performance metric, which quantifies the probability that the signal falls below a specified threshold, leading to a momentary loss of connectivity [7]. While the outage probability is essential to understanding the reliability of a system, it focuses on the occurrence of outage events without considering their duration. More meaningful second-order statistics of multipath fading channels include the level crossing rate (LCR) and average fade duration (AFD). The LCR indicates how frequently the envelope crosses a specific threshold, whereas the AFD measures the duration for which the envelope remains below a given threshold. These statistics play a significant role in characterizing the dynamic behavior and reliability of wireless communication systems, offering valuable insights into the temporal aspects of signal fluctuations and outage occurrences. Several studies have investigated LCR and AFD for various environments and under different assumptions [8]–[14]. These metrics are particularly essential for testing the performance of 6G wireless systems [15]. Another metric, the outage contiguous duration, has been recently developed and defined as the average time duration during which the signal envelope contiguously remains within a bounded amplitude interval, as described in [16]. While these metrics provide valuable information, it is of practical interest to study the distribution of the fading duration rather than focusing only on its average value. Previous research has only calculated the average time during which the signal stays below a given threshold, and the density of this duration has not been thoroughly explored.

The present study employs dynamical models to investigate the distribution of fade duration within a fixed observation interval. This use of dynamical models is crucial for accurately representing real-world wireless channels. Unlike static models where channel parameters are assumed random but constant throughout observation and estimation phases [17]–[20], actual wireless channels exhibit dynamic behavior. Research has advanced toward stochastic models to address these challenges, offering a better understanding of the dynamic behavior of wireless channels and enhanced modeling accuracy to match real-world conditions [21]–[24].

Notably, stochastic differential equations (SDEs) form a fundamental and robust framework for modeling dynamic systems subject to random fluctuations. Several studies have successfully employed SDEs to model multipath fading channels [25]–[30]. In particular, the research presented in [26] introduced a dynamic modeling approach for mobile-to-mobile channels, where system parameters were identified from received signal measurements. Additionally, in [30], SDEs were leveraged to model power loss and propose optimal power control algorithms based on the developed models. Furthermore, Lévy induced SDE network was recently proposed in [31] to capture the stochastic and rapid changes of wireless channels.

In this work, we leverage established SDE models for the inphase and quadrature components of the signal [25], [29], enabling a comprehensive analysis of fade duration in dynamic wireless environments. More precisely, we estimate the complementary cumulative distribution function (CCDF) of the fade duration. The problem is equivalent to computing the probability that the fade duration exceeds some limit, and by varying this limit across the observation time interval, we obtain an approximation of the CCDF. In this context, Monte

Eya Ben Amar, Raúl Tempone and Mohamed-Slim Alouini are with King Abdullah University of Science and Technology (KAUST), CEMSE division, Thuwal 23955-6900, Saudi Arabia (email: eya.benamar@kaust.edu.sa; raul.tempone@kaust.edu.sa; slim.alouini@kaust.edu.sa).

Nadhir Ben Rached is with the School of Mathematics, University of Leeds, Leeds, UK (email: N.BenRached@leeds.ac.uk).

Raúl Tempone is also an Alexander von Humboldt Professor in Mathematics for Uncertainty Quantification, RWTH Aachen University, 52062 Aachen, Germany.

This article has been accepted for publication in IEEE Transactions on Wireless Communications. This is the author's version which has not been fully edited and content may change prior to final publication. Citation information: DOI 10.1109/TWC.2025.3536615

Carlo (MC) simulations are an effective tool to estimate such probabilities.

In specific scenarios, it becomes rare for the fade duration to exceed a high limit. In practice, it is more desirable for the system to stay above a fixed threshold during the observation interval. Consequently, estimating the right tail of the CCDF of the fade duration takes on the role of calculating rare event probabilities. In this context, the crude MC method falls short in estimating such probabilities and necessitates an impractical number of simulations for accurate estimations [32]. Therefore, it is necessary to use appropriate variance-reduction techniques. Importance sampling (IS) is among the most popular variance-reduction techniques that deliver precise estimates of rare event probabilities with a reduced number of simulations [32]. We propose a dynamic IS approach formulated via stochastic optimal control. The feasibility of this optimal IS scheme necessitates developing a lower-dimensional SDE for the square envelope. The work in [29] captured the dynamics of the square envelope via a one-dimensional (1D) SDE, using Lévy's characterization theorem. However, it was established that this model remains valid exclusively under Rayleigh fading conditions.

The contributions of this paper are listed as follows:

1) We employ a MC estimator to estimate the CCDF of the fade duration. Additionally, we analyze its behavior under varying channel parameters.
2) We propose an IS estimator for efficiently estimating the right tail of the CCDF of the fade duration, highlighting the necessity of a 1D SDE for optimal estimation.
3) Using Markovian projection (MP), we derive a 1D SDE for the square envelope based on the two-dimensional (2D) SDE for the in-phase and quadrature components of the signal. We investigate three cases where the envelope is asymptotically Rayleigh, Rician, or Hoyt.
4) We present numerical results for the CCDF of fade duration, employing the optimal IS estimator in the Rayleigh scenario and a suboptimal IS estimator in the Rice scenario, demonstrating how IS significantly reduces the number of simulations required for accurate tail estimation of the CCDF.

The paper is structured as follows: Section II introduces the fading duration metric and proposes a MC estimator to estimate its complementary CCDF. Section III presents the motivation for the need for variance reduction techniques and proposes an IS estimator to efficiently estimate the tail of the CCDF. Section IV is dedicated to modeling the signal envelope of time-varying wireless channels using 1D SDE, assessing three cases: Rayleigh, Rice, and Hoyt fading. Finally, Section V provides numerical results for the CCDF of the fade duration in the Rayleigh and Rice cases using IS estimators.

II. Fading Duration

A. Channel Model

In our study, we employed well-established SDE models to describe the random variations of signal components in the time domain. Specifically, the work presented in [25] focuses on the Rayleigh fading scenario, starting from models that utilize SDEs for phase changes and ultimately modeling the in-phase and quadrature components using Ornstein-Uhlenbeck SDEs. In particular, the phase changes $\varphi^{(k)}(s)$ satisfy the following equation:

$$d\varphi^{(k)}(s) = B^{1/2} dW^{(k)}(s), \tag{1}$$

where $W^{(k)}$ are independent Wiener processes, and B is a constant with the dimension of frequency, which determines the correlation timescale for the component phase processes $\varphi^{(k)}(s)$. Based on (1), [25] modeled the in-phase $I(s)$ and quadrature $Q(s)$ as follows:

$$\begin{cases} dI(s) = -\dfrac{1}{2} BI(s)ds + \dfrac{\sqrt{2}}{2} B^{\frac{1}{2}} \sigma dW^{(I)}(s), \\ dQ(s) = -\dfrac{1}{2} BQ(s)ds + \dfrac{\sqrt{2}}{2} B^{\frac{1}{2}} \sigma dW^{(Q)}(s), \end{cases} \tag{2}$$

where $W^{(I)}(s)$ and $W^{(Q)}(s)$ denote independent Wiener processes, and σ^2 is the variance of the scattered electric field $\varepsilon(s) = \sum \exp\left[i\varphi^{(k)}(s)\right]$. Furthermore, the SDE framework proposed in [29] addresses the in-phase and quadrature components for Rayleigh, Rician, and Nakagami-m fading scenarios. These fading environments, as highlighted in [6], remain pertinent in modern Terahertz wireless communications. The models in [29] and [25] assume first-order Markovian fading channels, a condition further substantiated by recent studies [33]–[37].

Building on these models, we extend the framework to the more general Beckmann case, where the in-phase and quadrature components are independent Gaussian random processes with distinct time-varying means and variances. We express $I(s)$ and $Q(s)$ as solutions to the following generalized Ornstein-Uhlenbeck SDEs for $0 \leq t < s < T$, where t is the initial time, and T is the final time:

$$\begin{cases} dI(s) = k_1 \left(\theta_1 - I(s)\right) ds + \beta_1 dW^{(I)}(s), \\ dQ(s) = k_2 \left(\theta_2 - Q(s)\right) ds + \beta_2 dW^{(Q)}(s), \quad t < s < T \\ I(t) = I_t \\ Q(t) = Q_t, \quad 0 \leq t < T, \end{cases} \tag{3}$$

where k_1, k_2, θ_1, θ_2, β_1, and β_2 are constants in $\mathbb{R}$. From the statistics of $I(s)$ and $Q(s)$, derived in Appendix A, $I(s)$ and $Q(s)$ represent Gaussian variables with asymptotic means θ_1 and θ_2 and asymptotic variances $\frac{\beta_1^2}{2k_1}$ and $\frac{\beta_2^2}{2k_2}$, respectively.

We let $X(s) = \sqrt{I^2(s) + Q^2(s)}$ be the received signal envelope, where $X(s)$ can have a Rayleigh, Rice, Hoyt, or Beckmann distribution depending on the absence or presence of a strong line of sight [38]. More precisely,

- If $\theta_1 = \theta_2 = 0$, $k_1 = k_2 = k$, and $\beta_1 = \beta_2 = \beta$, then $X(s)$ has an asymptotic Rayleigh distribution with the parameter $\frac{\beta}{\sqrt{2k}}$.
- If $k_1 = k_2 = k$ and $\beta_1 = \beta_2 = \beta$, then $X(s)$ has an asymptotic Rice distribution with the parameters $(\sqrt{\theta_1^2 + \theta_2^2}, \frac{\beta}{\sqrt{2k}})$.
- If $\theta_1 = \theta_2 = 0$, then $X(s)$ has an asymptotic Nakagami-q (Hoyt) distribution [39] with the shape parameter $q = \frac{\beta_2}{\beta_1}\sqrt{\frac{k_1}{k_2}}$ and $\mathbb{E}[X^2] = \frac{\beta_1^2}{2k_1} + \frac{\beta_2^2}{2k_2}$.
- If $\theta_1 \neq \theta_2 = 0$, $k_1 \neq k_2$, and $\beta_1 \neq \beta_2$, then $X(s)$ has an asymptotic Beckmann distribution.

This article has been accepted for publication in IEEE Transactions on Wireless Communications. This is the author's version which has not been fully edited and content may change prior to final publication. Citation information: DOI 10.1109/TWC.2025.3536615

B. Problem Formulation

We let $Z(T)$ be the time during which the received signal envelop $X(s)$ remains below a given threshold $\gamma \in \mathbb{R}_+$, in the time interval $[0, T]$. In other words, $Z(T)$ indicates the fading time of the signal in the period $[0, T]$. Moreover, $Z(T)$ is the solution at final time T of the following ordinary differential equation:

$$\begin{cases} dZ(s) = \mathbb{1}_{\{X(s)<\gamma\}} ds, \quad t < s < T \\ Z(t) = z, \quad 0 \le t < T, \end{cases} \tag{4}$$

where $\mathbb{1}_{\{X(s)<\gamma\}}$ is an indicator function that equals 1 if $\{X(s) < \gamma\}$ and 0 otherwise.
Therefore,

$$Z(T) = z + \int_t^T \mathbb{1}_{\{X(s)<\gamma\}} ds. \tag{5}$$

The goal is to determine the distribution of $Z(T)$. To achieve this, we calculated the CCDF of $Z(T)$ given by $P(Z(T) > w|X(t) = x, Z(t) = z)$, for $0 \le w \le T$. First, we formulated the problem as a multidimensional SDE:

$$\begin{cases} dI(s) = k_1 (\theta_1 - I(s))\, ds + \beta_1 dW^{(I)}(s), \\ dQ(s) = k_2 (\theta_2 - Q(s))\, ds + \beta_2 dW^{(Q)}(s), \\ dZ(s) = f(I(s), Q(s)) ds, \quad t < s < T, \\ I(t) = I_t, \\ Q(t) = Q_t, \\ Z(t) = z, \quad 0 \le t < T, \end{cases} \tag{6}$$

where $f(x, y) = \mathbb{1}_{\{x^2+y^2<\gamma^2\}}$. The quantity of interest, for an initial time t and initial states I_t, Q_t, and z, can be expressed as follows:

$$\begin{aligned} &P(Z(T) > w|I(t) = I_t, Q(t) = Q_t, Z(t) = z) \\ &= \mathbb{E}[g_w(Z(T)) \mid I(t) = I_t, Q(t) = Q_t, Z(t) = z], \end{aligned} \tag{7}$$

where $g_w(x) = \mathbb{1}_{\{x>w\}}$ and $\mathbb{E}[.]$ denotes the expected value. The distribution of $Z(T)$ is unknown; thus, it is not possible to obtain a closed form of the conditional expectation in (7). Instead, we only have access to samples of $Z(T)$, obtained by numerically solving the SDE in (6). In this case, one approach to estimating the CCDF is to use MC simulations.

C. Monte Carlo Estimator

Obtaining analytical solutions to complex SDEs may not always be possible. In practice, numerical methods, such as the Euler–Maruyama scheme, are often used to approximate the solution and simulate the behavior of the system over time. The Euler–Maruyama scheme provides a numerical approximation to the solution of the SDE over a discrete time interval [40]. We consider a time discretization $0 = t_0 < t_1 < \ldots < t_N = T$, and define I^N, Q^N, and Z^N as the discretized representations of the states I, Q, and Z, respectively. Given an initial value I_0 and Q_0, the Euler–Maruyama scheme updates the state variables $I^N(t)$, $Q^N(t)$, and $Z^N(t)$ at each time step $\Delta t = \frac{T}{N}$ as follows:

$$I^N(0) = I_0, Q^N(0) = Q_0, Z^N(0) = 0, \tag{8}$$

and for $n = 0, \ldots, N-1$,

$$\begin{aligned} I^N(t_{n+1}) &= I^N(t_n) + k_1 \left(\theta_1 - I^N(t_n)\right) \Delta t + \beta_1 \Delta W_n^{(I)}, \\ Q^N(t_{n+1}) &= Q^N(t_n) + k_2 \left(\theta_2 - Q^N(t_n)\right) \Delta t + \beta_2 \Delta W_n^{(Q)}, \\ Z^N(t_{n+1}) &= Z^N(t_n) + f(I^N(t_n), Q^N(t_n)) \Delta t, \end{aligned} \tag{9}$$

where $\Delta W_n^{(I)}$ and $\Delta W_n^{(Q)}$ are independent Gaussian random variables (RVs) with distribution $\mathcal{N}(0, \Delta t)$.

By solving the SDE in (6) M times, we obtain M independent samples $\{Z^{(k)}(T)\}_{k=1}^M$ of $Z(T)$. Finally,

$$\mathbb{E}[g_w(Z(T))] \approx \frac{1}{M} \sum_{k=1}^M g_w\left(Z^{(k)}(T)\right). \tag{10}$$

Fig. 1 presents the numerical results of the estimation of the CCDF in the Rayleigh case using the MC estimator. We investigate two scenarios: when the process starts above the threshold i.e. $I_0 = Q_0 = 1$, and when the process begins below the threshold i.e. $I_0 = Q_0 = 0$. In the case where the process is initially above the threshold, Fig. 1 reveals an interesting observation: discontinuity occurs at $w = 0$. In fact, $P(Z(T) = 0) = 0.17 \ne 0$, representing the size of the jump of the represented CCDF. This implies that $Z(T)$ is a mixed RV with a jump at w equal to zero. This phenomenon is explained by the fact that there is a non-zero probability that the signal will remain above the threshold for the entire duration of the interval $[0, T]$. This is possible when the process starts above the threshold and with specific parameters.

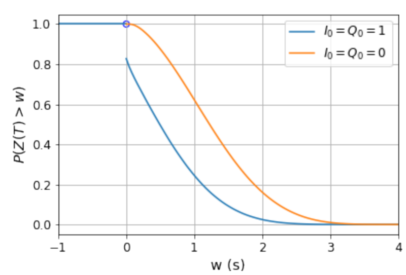

Fig. 1: Estimated complementary cumulative distribution function (CCDF) in the Rayleigh case using the Monte Carlo (MC) method with the following parameters: $T = 4$, $N = 100$, $k = 0.5$, $\beta = \frac{\sqrt{2}}{2}$, and $\gamma = 0.5$.

III. Importance Sampling for Right-Tail Estimation

A. Motivation

When estimating $P(Z(T) > w)$, it becomes evident that the MC method tends to estimate a probability of zero when w approaches T from the left. However, we anticipate that the actual value is extremely small but not precisely zero, given that the occurrence of the event $\{Z(T) > w\}$ is rare when $T - w$ is small. Moreover, the MC estimations tend to be inaccurate for such infrequent events. To illustrate this, we calculated the relative error, defined using the central limit theorem as follows:

$$\epsilon_{MC} = C \frac{\sqrt{P(Z(T) > w)(1 - P(Z(T) > w))}}{\sqrt{M_{MC}} P(Z(T) > w)}, \tag{11}$$

where C denotes the confidence constant, equal to 1.96 for the 95 % confidence interval, and M_{MC} represents the number of samples for the MC estimator.

This article has been accepted for publication in IEEE Transactions on Wireless Communications. This is the author's version which has not been fully edited and content may change prior to final publication. Citation information: DOI 10.1109/TWC.2025.3536615

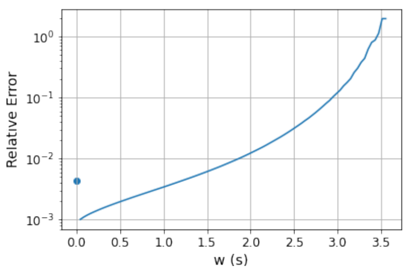

Fig. 2: Relative error of the Monte Carlo (MC) estimator of $P(Z(T) > w)$ with the following parameters $T = 4$, $N = 100$, $I_0 = Q_0 = 1$, $k = 0.5$, $\beta = \frac{\sqrt{2}}{2}$, and $\gamma = 0.5$.

Fig. 2 displays the relative error for the range of w, using $M_{MC} = 10^6$. The relative error significantly increases approaching the right tail. This phenomenon implies that the MC method requires more samples to achieve a given relative error as the value of w increases. Notably, even with a sample size of 10^6, MC struggles to estimate $P(Z(T) > w)$ accurately for $w > 3.5$. Consequently, we must employ variance-reduction techniques to minimize the required number of samples for estimating the right tail of the CCDF. We employed IS as one such technique.

Remark 1. *Given the discontinuity in the CCDF when $I_0 = Q_0 = 1$, as shown in Fig. 1, we have calculated the relative error in estimating the size of the jump at $w = 0$ and plotted it as a scatter point in Fig. 2. It is important to note that, for certain parameter settings, the size of the jump becomes very small, and consequently, leading to a high relative error. For instance, by replacing $k = 0.5$ with $k = 5$, we find that $P(Z(T) = 0) \approx 10^{-6}$, resulting in a substantial increase in the relative error for estimating the jump in the CCDF (approximately 195%). In such cases, the utilization of variance-reduction techniques becomes indispensable to achieve a highly accurate estimation of $P(Z(T) = 0)$. This work focuses on rare events in the right tails of the distribution, while future research may address specific cases where $P(Z(T) = 0)$ is exceedingly small.*

B. Importance Sampling

We present the idea of IS in the general case before applying it to SDEs. We consider the estimation of $\mathbb{E}[g(X)]$, where X is an RV with probability density function (PDF) f, and g is a given function. In scenarios where g takes the form of an indicator function, signifying probability estimation, the region of rare events occurs when this quantity becomes extremely small. In this case, standard MC simulations require considerable number of samples to obtain accurate estimates. In addition, the IS method is among the most popular variance-reduction techniques used to overcome the failure of naive MC simulations and reduce the computational work [41]–[43]. The idea is to modify the sampling distribution so that the rare event is generated with a higher probability than under the original distribution [32]. We consider a new PDF $\tilde{f}$ such that

$$supp\Big\{f(.)g(.)\Big\} \quad \subset \quad supp\{\tilde{f}(\cdot)\}, \tag{12}$$

where $supp\{f\} = \{x \in \mathbb{R}^d \mid f(x) \neq 0\}$. The IS technique consists of writing the quantity of interest as follows:

$$\begin{aligned}\mathbb{E}[g(X)] &= \int_{\mathbb{R}^d} g(x)f(x)dx \\ &= \int_{\mathbb{R}^d} g(x)\frac{f(x)}{\tilde{f}(x)}\tilde{f}(x)dx = \mathbb{E}_{\tilde{f}}\left[\tilde{g}\left(X\right)\right],\end{aligned} \tag{13}$$

where $\tilde{g}\left(x\right) = g\left(x\right)\frac{f(x)}{\tilde{f}(x)}$, and $\mathbb{E}_{\tilde{f}}$ is the expectation under which the RV X has the PDF $\tilde{f}$. Then, the IS estimator is

$$\mathcal{A}_{IS} = \frac{1}{M}\sum_{k=1}^{M}\tilde{g}\left(X^{(k)}\right), \tag{14}$$

where $\{X^{(k)}\}_{k=1}^{M}$ represents independent realizations of X sampled according to $\tilde{f}$.

In the context of SDEs, if $X(s) \in \mathbb{R}^d$ solves the following SDE:

$$\begin{cases} dX(s) = a(s, X(s))ds + b(s, X(s))dW(s), 0 < s < T \\ X(0) = x_0, \end{cases} \tag{15}$$

and we aim to estimate $\mathbb{E}\left[g\left(X(T)\right)\right]$, the change of measure in the IS method is performed in the path space induced by the Wiener process. We apply a change of measure to the SDE in (15) such that we minimized the variance of the MC estimator. We formulate the problem of finding an optimal change of measure as a stochastic optimal control problem. To better understand this, we let $X^N(t)$ be the forward Euler–Maruyama approximation of the proposed process $X(t)$. Then,

$$\begin{cases} X^N(t_{n+1}) = X^N(t_n) + a(X^N(t_n), t_n)\Delta t \\ \qquad\qquad +b(X^N(t_n), t_n)\sqrt{\Delta t}\epsilon_n, \quad n = 0, \ldots, N-1 \\ X^N\left(t_0\right) = X(0) = x_0, \end{cases} \tag{16}$$

where $\epsilon_n, n = 1, \cdots, N$ are independent and identically distributed standard normal vectors. We let $\zeta_n = \zeta(X^N(t_n), t_n)$ be the control at the time step t_n and we propose a measure change on each ϵ_n, of the following form:

$$\hat{\epsilon}_n = \sqrt{\Delta t}\zeta_n + \epsilon_n. \tag{17}$$

Therefore, the new path X_ζ^N satisfies

$$\begin{cases} X_\zeta^N(t_{n+1}) = X^N(t_n) + \left(a(X_\zeta^N(t_n), t_n) + b(X_\zeta^N(t_n), t_n)\zeta_n\right)\Delta t \\ \qquad\qquad +b(X_\zeta^N(t_n), t_n)\sqrt{\Delta t}\epsilon_n \\ X_\zeta^N(t_0) = X^N\left(t_0\right) = x_0. \end{cases} \tag{18}$$

The objective is to minimize the variance of the resulting estimator. As the IS estimator is unbiased, minimizing the variance is equivalent to minimizing the second moment. To maintain unbiasedness, we introduced the likelihood as follows:

$$L_n\left(\hat{\epsilon}_n\right) = \exp\left\{-\frac{1}{2}\left\|\hat{\epsilon}_n\right\|^2\right\}\exp\left\{\frac{1}{2}\|\hat{\epsilon}_n - \sqrt{\Delta t}\zeta_n\|^2\right\}. \tag{19}$$

After replacing the expression of $\hat{\epsilon}_n$, the likelihood function becomes

$$L_n\left(\epsilon_n\right) = \exp\left\{-\frac{1}{2}\Delta t\left\|\zeta_n\right\|^2 - \sqrt{\Delta t}\left\langle\epsilon_n, \zeta_n\right\rangle\right\}, \tag{20}$$

where $\langle\cdot,\cdot\rangle$ is the dot product between two vectors, and $||.||$ is the Euclidean norm of the vector. Finally, the quantity of interest can be expressed as follows:

$$\mathbb{E}\left[g\left(X^N(T)\right)\right] = \mathbb{E}\left[g\left(X_\zeta^N(T)\right)\prod_{n=0}^{N-1}L_n\left(\epsilon_n\right)\right]. \tag{21}$$

This article has been accepted for publication in IEEE Transactions on Wireless Communications. This is the author's version which has not been fully edited and content may change prior to final publication. Citation information: DOI 10.1109/TWC.2025.3536615

The objective is to minimize the second moment; thus, the cost function is defined as follows:

$$C_{t,x}(\zeta_0,\cdots,\zeta_{N-1}) = \mathbb{E}\left[g^2\left(X_\zeta^N(T)\right)\prod_{n=0}^{N-1} L_n^2(\epsilon_n) \mid X_\zeta^N(t)=x\right]$$
$$=\mathbb{E}\left[g^2\left(X_\zeta^N(T)\right)\right.$$
$$\left.\times\prod_{n=0}^{N-1}\exp\left\{-\Delta t\|\zeta_n\|^2 - 2\langle\epsilon_n,\zeta_n\rangle\sqrt{\Delta t}\right\} \mid X_\zeta^N(t)=x\right]. \tag{22}$$

Taking the limit as $\Delta t \to 0$ leads to the following:

$$C_{t,x}(\zeta) = \mathbb{E}\left[g^2\left(X_\zeta(T)\right)\exp\left\{-\int_t^T \|\zeta(s,X_\zeta(s))\|^2 \, \mathrm{d}s\right.\right.$$
$$\left.\left.-2\int_t^T\langle\zeta(s,X_\zeta(s)),\mathrm{d}W(s)\rangle\right\} \mid X_\zeta(t)=x\right], \tag{23}$$

where ζ is the IS parameter that defines the measure change and X_ζ is subject to the controlled SDE dynamics

$$\begin{cases} \mathrm{d}X_\zeta(s) = \left(a(s,X_\zeta(s)) + b(s,X_\zeta(s))\,\zeta(s,X_\zeta(s))\right)\mathrm{d}s \\ \qquad\qquad +b(s,X_\zeta(s))\,\mathrm{d}W(s), \quad 0<s<T \\ X_\zeta(t)=X(t)=x, \quad 0\le t<T. \end{cases} \tag{24}$$

We defined the value function as follows:

$$u(t,x) = \min_{\zeta\in\mathcal{B}} C_{t,x}(\zeta), \tag{25}$$

where $\mathcal{B}$ is the set of admissible Markov controls. One conceivable approach to identifying a suitable control ζ involves the application of a parametric family of change of measure and solving the optimization problem in (25) to determine the optimal parameters that provide the optimal control ζ within the preselected class of measures. In contrast, if the aim is to determine the optimal control in the full spectrum of possible Markov controls, it is best to apply Theorem 1 [44].

Theorem 1. *We assume that the value function $u(t,x)$ defined in (25) is bounded and smooth and let D represent the support of u, meaning that $u(t,x)$ is nonzero for $(t,x)\in D$. Then, $u(t,x)$ solves the following PDE:*

$$\begin{cases} \partial_t u + \sum_{i=1}^d a_i\partial_{x_i}u + \frac{1}{2}\sum_{i,j,k=1}^d b_{ik}b_{jk}\partial_{x_ix_j}u \\ -\frac{1}{4u}\sum_{i=1}^d\left(\sum_{j=1}^d \partial_{x_j}u\, b_{ij}\right)^2 = 0, \quad (t,x)\in D \\ u(T,.)=g^2, \end{cases} \tag{26}$$

where a_i denotes the ith component of the drift vector a, b_{ij} represents the element in the ith row and jth column of matrix b, $\partial_{x_i}u$ denotes the derivative of u with respect to the ith component of vector x, and $\partial_{x_ix_j}u$ is the second derivative of u with respect to the ith and jth components of vector x. The optimal control is computed as follows:

$$\zeta^*(t,x) = \frac{1}{2}b(t,x)\nabla\log u(t,x), \tag{27}$$

where ∇ denotes the gradient vector.

Proof: See the proof in [45]. ∎

We assume that g does not change the sign. If we introduce the change of variable $u(t,x)=v^2(t,x)$ and substitute $u(t,x)$ with $v^2(t,x)$ in equation (26), we can deduce, as developed in [45], that v exactly solves the Kolmogorov backward equations (KBEs) given by

$$\begin{cases} \partial_t v + \sum_{i=1}^d a_i\partial_{x_i}v + \frac{1}{2}\sum_{i,j,k=1}^d b_{ik}b_{jk}\partial_{x_ix_j}v = 0, \ t<T, \\ v(T,.)=g. \end{cases} \tag{28}$$

The KBE formulates a deterministic PDE whose solution may be written in the form of an expectation value of a terminal condition [46]. The solution of the KBE (28) corresponds to the conditional expectation $\mathbb{E}[g(X(T)) \mid X(t)=x]$. The quantity $u(t,x)$ defined in (25) represents the second moment of the IS estimator. Given that $v(t,x)$ precisely represents the quantity to estimate, by employing the optimal control (27), the second moment of the IS estimator equals the square of the first moment, resulting in a variance of zero.

Remark 2. *Solving the KBE in (28) suffers from the curse of dimensionality, wherein the computational cost escalates exponentially as the dimensionality d increases. Specifically, applying the optimal change of measure on the SDE in (6) necessitates solving a PDE with three spatial dimensions and one temporal dimension, which can be computationally expensive and, given limited resources, may even become infeasible. One potential solution is to derive an SDE for the square envelope $R(s)=I^2(s)+Q^2(s)$, and then apply the change of measure to the SDE for (R,Z) instead of (I,Q,Z). This approach reduces the dimensionality by one, making solving the PDE in (28) computationally feasible.*

IV. One-Dimensional Stochastic Differential Equations for the Square Envelop Using Markovian Projection

Based on the model in (3), the work in [29] has modeled the dynamics of the square envelope $R(s)$, subject to short-term fading, by the following SDE:

$$\begin{cases} dR(s) = (c_1 - c_2R(s))\,ds + c_3\sqrt{R(s)}dW(s), \quad t<s<T \\ R(t)=R_t, \quad 0\le t<T, \end{cases} \tag{29}$$

where c_1, c_2, and c_3 are constants in $\mathbb{R}$. It used Ito's differential rule [47] and Lévy's characterization theorem [48], to transition from a 2D SDE for I and Q to a 1D Markovian SDE for R. The validity of the model in (29) has been established only in the Rayleigh case. In this work, we employ MP to derive a lower-dimensional, Markovian SDE for $R(s)$ in more general cases, such as when the envelope $X(s)$ is asymptotically Rayleigh, Rician, or Hoyt.

A. Markovian Projection

The MP, in the context of SDEs, represents a powerful technique to project a high-dimension SDE into a lower-dimensional one, while preserving the marginal distribution. The following lemma details the dynamics of the projected SDE:

Lemma 1. *Markovian projection [49]*
We let $X\in\mathbb{R}^d$ solve

$$\begin{cases} \mathrm{d}X(t) = a(t,X(t))\mathrm{d}t + b(t,X(t))\mathrm{d}W(t), \quad 0<t<T \\ X(0)=x_0, \quad x_0\in\mathbb{R}^d, \end{cases} \tag{30}$$

This article has been accepted for publication in IEEE Transactions on Wireless Communications. This is the author's version which has not been fully edited and content may change prior to final publication. Citation information: DOI 10.1109/TWC.2025.3536615

and we consider the non-Markovian process $S = PX$, where $S \in \mathbb{R}^{\bar{d}}$ and $P^T = \left(P_1^T, \cdots, P_{\bar{d}}^T\right)^T$ represents the projection matrix onto a dimension $1 \leq \bar{d} < d$.

We let $\bar{S}^{(x_0)} \in \mathbb{R}^{\bar{d}}$ solve for $t \in [0, T]$

$$\begin{cases} d\bar{S}^{(x_0)}(t) = \bar{a}^{(x_0)}\left(t, \bar{S}^{(x_0)}(t)\right) dt + \bar{b}^{(x_0)}\left(t, \bar{S}^{(x_0)}(t)\right) d\bar{W}(t), \\ \bar{S}^{(x_0)}(0) = Px_0, \end{cases} \tag{31}$$

where $\bar{W}$ denotes a Wiener process, independent of W. The drift and diffusion coefficients of the surrogate process $\bar{S}^{(x_0)}$ are determined for $1 \leq i, j \leq \bar{d}$ as follows:

$$\begin{aligned} \bar{a}^{(x_0)}(t, s) &= \mathbb{E}\left[Pa(t, X(t)) \mid PX(t) = s, X(0) = x_0\right] \\ \left(\bar{b}\bar{b}^T\right)_{ij}^{(x_0)}(t, s) &= \mathbb{E}\left[\left(P_i^T bb^T P_j\right)(t, X(t)) \mid PX(t) = s, X(0) = x_0\right]. \end{aligned} \tag{32}$$

Then, $S(t)|_{\{X(0)=x_0\}} = PX(t)|_{\{X(0)=x_0\}}$ and $\bar{S}^{(x_0)}(t)$ have the same conditional distribution for all $t \in [0, T]$.

Proof: See the proof in [49] for similar derivations. ■

In this context, we employed MP by taking $X = (I, Q, R)^T$, $P = (0, 0, 1)^T$, and $S = R$, where I and Q are solutions of (3), and $R = I^2 + Q^2$. The MP of R, denoted as $\bar{R}$, is obtained by solving the following SDE:

$$\begin{cases} \mathrm{d}\bar{R}(s) &= \bar{a}(s, \bar{R})\mathrm{d}s + \bar{b}(s, \bar{R})\mathrm{d}W(s), \quad 0 < s < T \\ \bar{R}(0) &= R(0). \end{cases} \tag{33}$$

The determination of the drift $\bar{a}(s, \bar{R})$ and diffusion $\bar{b}(s, \bar{R})$ components relies on the application of MP Lemma 1 and depends on the characteristics of the fading environment, whether Rayleigh, Rice, or Hoyt.

B. Rayleigh Case

When the Ornstein–Uhlenbeck processes $I(s)$ and $Q(s)$ are identically distributed, and do not have a long-term mean adjustment, the SDE (3) can be expressed as (2), where $B = 2k$ and $\sigma = \frac{\beta}{\sqrt{k}}$. Using Ito's formula, $R(s)$ solves the following non-Markovian SDE:

$$\begin{cases} \mathrm{d}R(s) = B\left(\sigma^2 I^2(s) - Q^2(s)\right)\mathrm{d}s \\ \qquad\qquad + \sqrt{2B}\sigma[I(s) \quad Q(s)]\begin{bmatrix} \mathrm{d}W^I(s) \\ \mathrm{d}W^Q(s) \end{bmatrix}, \\ R(0) = I^2(0) + Q^2(0). \end{cases} \tag{34}$$

From MP Lemma 1, the projected process $\bar{R}$ solves (33) with the projected drift coefficient:

$$\begin{aligned} \bar{a}(s, r) &= \mathbb{E}\left[B\left(\sigma^2 - I^2(s) - Q^2(s)\right) \mid R(s) = r, I(0) = I_0, Q(0) = Q_0\right] \\ &= B\left(\sigma^2 - r\right), \end{aligned} \tag{35}$$

and the projected diffusion coefficient:

$$\begin{aligned} \bar{b}^2(s, r) &= \mathbb{E}\left[2B\sigma^2\left(I^2(s) + Q^2(s)\right) \mid R(s) = r, I(0) = I_0, Q(0) = Q_0\right] \\ &= 2B\sigma^2 r \\ \Rightarrow \bar{b}(s, r) &= \sigma\sqrt{2Br}. \end{aligned} \tag{36}$$

Therefore, for $0 < s < T$, (33) can be written as

$$\begin{cases} d\bar{R}(s) = B\left(\sigma^2 - \bar{R}(s)\right)ds + \sigma\sqrt{2B\bar{R}(s)}dW(s), \\ \bar{R}(0) = R(0). \end{cases} \tag{37}$$

This result precisely corresponds to the SDE form stated in (29). Consequently, we substantiated the validity of the proposed model, derived using MP rather than Lévy's characterization theorem.

We studied the properties of the projected process $\bar{R}$. First, we checked the stationary distribution of $\bar{R}$ using the Fokker–Plank equation. The limit distribution $p(.)$ of the projected process $\bar{R}$ satisfies

$$\frac{\partial}{\partial y}(yp(y)) = \left(1 - \frac{y}{\sigma^2}\right)p(y), \quad y > 0. \tag{38}$$

Moreover, the solution of (38) is

$$p(y) = \frac{1}{\sigma^2}e^{\frac{-y}{\sigma^2}}, \quad y > 0. \tag{39}$$

Therefore, $\bar{R}(s)$ is an asymptotic exponential distribution with parameter $\frac{1}{\sigma^2}$, which is the exact asymptotic distribution of $R(s)$. We also calculated the statistics of $\bar{R}$ in Appendix A. The asymptotic means and variances are the same as the statistics of R. Furthermore, the expression for the autocorrelation (78) is nonconstant in the stationary regime, in contrast to the Clark model. Instead, it exhibits the same exponentially decaying form as the autocorrelation of the fading in the extended Clark model under the condition of a zero Doppler shift, as developed in [22].

We solved the original SDE (3) and the projected SDE (37) and compared in Fig. 3 the histograms of $\bar{R}(T)$ and $I(T)^2 + Q(T)^2$. The samples of $\bar{R}(T)$ produce a histogram that closely resembles $I(T)^2 + Q(T)^2$.

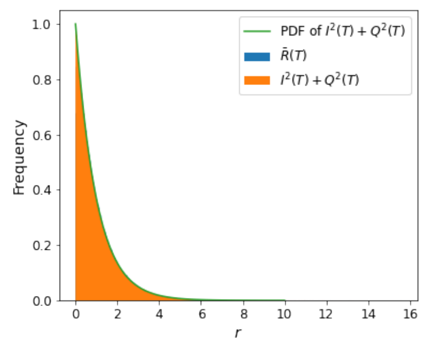

Fig. 3: Rayleigh Fading: Histogram of $\bar{R}(T)$ and $I(T)^2 + Q(T)^2$ using 10^6 samples with the following parameters: $T = 4$, $N = 100$, $I_0 = 0$, $Q_0 = 0$, $B = 1$, and $\sigma = 1$.

C. Rice Fading

As explained in Section II-A, when $I(s)$ and $Q(s)$ have a long-term mean adjustment θ, they solve the following SDE:

$$\begin{cases} dI(s) = k\left(\theta - I(s)\right)ds + \beta dW^{(I)}(s), \\ dQ(s) = k\left(\theta - Q(s)\right)ds + \beta dW^{(Q)}(s), \quad 0 < s < T \\ I(0) = I_0, \\ Q(0) = Q_0. \end{cases} \tag{40}$$

Using Ito's formula, $R(s)$ solves the following non-Markovian SDE, for $0 < s < T$,

$$\begin{cases} \mathrm{d}R(s) = \left(2k\theta(I(s) + Q(s)) - 2k(I^2(s) + Q^2(s)) + 2\beta^2\right)\mathrm{d}s \\ \qquad\qquad + \sqrt{2\beta}\sigma[I(s) \quad Q(s)]\begin{bmatrix} \mathrm{d}W^I(s) \\ \mathrm{d}W^Q(s) \end{bmatrix} \\ R(0) = I^2(0) + Q^2(0). \end{cases} \tag{41}$$

Applying Lemma 1, we find that the projected process $\bar{R}$ solves (33), with the projected drift:

$$\begin{aligned}\bar{a}(s,r) = \mathbb{E}\big[&2k\theta(I(s)+Q(s)) - 2k(I^2(s)+Q^2(s)) \\ &+2\beta^2 \mid R(s)=r, I(0)=I_0, Q(0)=Q_0\big],\end{aligned} \tag{42}$$

and the projected diffusion coefficient:

$$\begin{aligned}&\bar{b}^2(s,r) \\ &= 4\mathbb{E}\left[\beta^2(I^2(s)+Q^2(s)) \mid R(s)=r, I(0)=I_0, Q(0)=Q_0\right] \\ &= 4\beta^2 r \\ &\Rightarrow \bar{b}(s,r) = 2\beta\sqrt{r}.\end{aligned} \tag{43}$$

We let us assume that, initially, $I_0 = Q_0$; therefore, $I(s)$ and $Q(s)$ have the same Gaussian distribution at each time s, with a mean of:

$$m(s) = I_0\, e^{-ks} + \theta\left(1 - e^{-ks}\right), \tag{44}$$

and a variance of

$$\sigma^2(s) = \frac{\beta^2}{2k}\left(1 - e^{-2ks}\right). \tag{45}$$

Consequently,

$$\begin{aligned}\bar{a}(s,r) = 4k\theta\, &\mathbb{E}\left[I(s) \mid R(s)=r, I(0)=Q(0)=I_0\right] \\ &- 2kr + 2\beta^2.\end{aligned} \tag{46}$$

To derive an explicit expression for the drift $\bar{a}(s,r)$, we compute the conditional PDF $f_{I(s)|R(s)}(x \mid r)$ as described in Proposition 1. This computation allows us to determine the conditional expectation $\mathbb{E}\left[I(s) \mid R(s)=r, I(0)=Q(0)=I_0\right]$ as follows:

$$\mathbb{E}\left[I(s) \mid R(s)=r\right] = \int x f_{I(s)|R(s)}(x \mid r)dx. \tag{47}$$

Proposition 1. *If $(I(s), Q(s))$ solves (40), $R(s) = I^2(s) + Q^2(s)$, and $I_0 = Q_0$, then, for $r > x^2$,*

$$f_{I(s)|R(s)}(x \mid r) = \frac{\exp\left(\frac{x m(s)}{\sigma^2(s)}\right)\left(\frac{r-x^2}{m^2(s)}\right)^{-\frac{1}{4}}\mathcal{I}_{-\frac{1}{2}}\left(\frac{m(s)\sqrt{(r-x^2)}}{\sigma^2(s)}\right)}{\sqrt{2\pi}\sigma(s)\mathcal{I}_0\left(\frac{m(s)\sqrt{2r}}{\sigma^2(s)}\right)}, \tag{48}$$

where $\mathcal{I}_\mu$ is the modified Bessel function of the first kind with order μ.

Proof: See Appendix B. ■

However, if we use the expression (47) for the conditional expectation to formulate the drift (46), solving the SDE (37) becomes computationally expensive because we would need to evaluate the integral in (47) at each time step and for every sample. Alternatively, we can approximate the conditional expectation (47) using affine prediction. The conditional expectation can be approximated as follows:

$$\mathbb{E}[I(s) \mid R(s)=r] \simeq c_1(s)(r - \mathbb{E}[R(s)]) + c_2(s), \tag{49}$$

where $c_1(s) = \frac{\mathrm{Cov}(I(s),R(s))}{\mathrm{Var}(R(s))}$, and $c_2(s) = \mathbb{E}[I(s)]$. Here $\mathrm{Cov}(.,.)$ is the covariance, and $\mathrm{Var}(.)$ is the variance. Using the properties of the third and fourth moments of Gaussian RVs, we can demonstrate that:

$$\mathrm{Cov}(I(s),R(s)) = \mathrm{Cov}\left(I(s), I^2(s)+Q^2(s)\right) = 2m(s)\sigma^2(s), \tag{50}$$

$$\mathrm{Var}(R(s)) = \mathrm{Var}\left(I^2(s)+Q^2(s)\right) = 4m^2(s)\sigma^2(s) + 2\sigma^4(s). \tag{51}$$

Therefore,

$$\mathbb{E}[I(s) \mid R(s)=r] \simeq \frac{m(s)\sigma^2(s)\left(r - 2\left(\sigma^2(s)+m^2(s)\right)\right)}{4m^2(s)\sigma^2(s) + 2\sigma^4(s)} + m(s). \tag{52}$$

To assess the effectiveness of employing the affine approximation, we compared the exact drift $\bar{a}(s,r)$ obtained by evaluating the exact integral form for the conditional expectation, with the approximated drift $\tilde{a}(s,r)$ computed using affine prediction. The drifts $\bar{a}(s,r)$ and $\tilde{a}(s,r)$ depend on both the time s (which ranges over $[0,T]$) and the square envelope r (which can range from $[0,+\infty]$). To provide a clearer analysis, we fix the time s and plot both drifts as functions of r. The range of r can be adjusted based on the values of the square envelope for that specific time. To determine an appropriate range for r at each fixed time s, we display in Fig. 4 several samples of $I^2(s) + Q^2(s)$ as a function of s, obtained by solving the SDE in (40). For example, from Fig. 4, we observe that for a fixed time $s = 0.2$, the range of $I^2(s) + Q^2(s)$ is approximately $[0,2]$. Therefore, for $s = 0.2$, it is sufficient to plot the drifts $\bar{a}(s,r)$ and $\tilde{a}(s,r)$ as functions of r within the interval $[0,2]$. Fig. 5 shows $\bar{a}(s,r)$ and $\tilde{a}(s,r)$ plotted against r for different fixed values of $s \in \{0.2, 1, 3, 4\}$. The range of r for each fixed s is determined from Fig. 4.

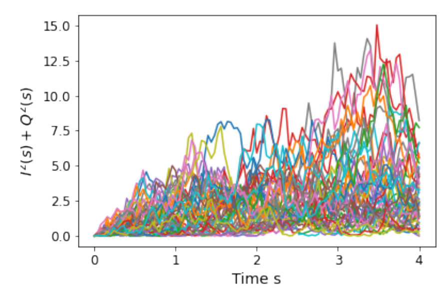

Fig. 4: Fifty samples of $I(s)^2 + Q(s)^2$ with the following parameters: $T = 4$, $N = 100$, $I_0 = 0$, $Q_0 = 0$, $k = 1$, $\theta = 1$, and $\beta = 1$.

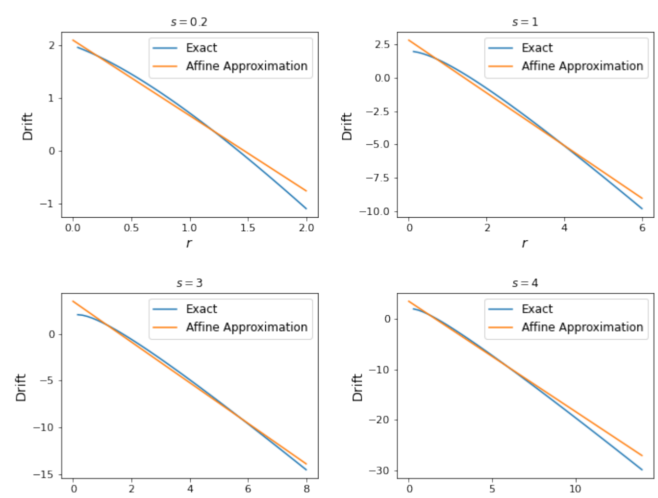

Fig. 5: Comparison of the exact and approximated drift with the following parameters: $T = 4$, $N = 100$, $I_0 = 0$, $Q_0 = 0$, $k = 1$, $\theta = 1$, and $\beta = 1$.

This article has been accepted for publication in IEEE Transactions on Wireless Communications. This is the author's version which has not been fully edited and content may change prior to final publication. Citation information: DOI 10.1109/TWC.2025.3536615

Fig. 5 reveals that the obtained affine expression is a good approximation for the conditional expectation. Therefore, we can use the linear approximation for the conditional expectation, and finally, the approximated drift $\tilde{a}(s,r)$ can be expressed as follows:

$$\tilde{a}(s,r) \approx 4k\theta \, \frac{m(s)\sigma^2(s)\left(r - 2\left(\sigma^2(s) + m(s)^2\right)\right)}{4m(s)^2\sigma^2(s) + 2\sigma^4(s)} + m(s) - 2kr + 2\beta^2, \tag{53}$$

where $m(s)$ and $\sigma^2(s)$ are given by (44) and (45).

To check the efficiency of the proposed projection, in Fig. 6 we plotted the histogram of the solution of the original SDE in (40) and the histogram of the solution of projected SDE in (33). The plot demonstrates that the paths of $I^2(T) + Q^2(T)$ and $\bar{R}(T)$ are almost the same; therefore, the approximation is robust.

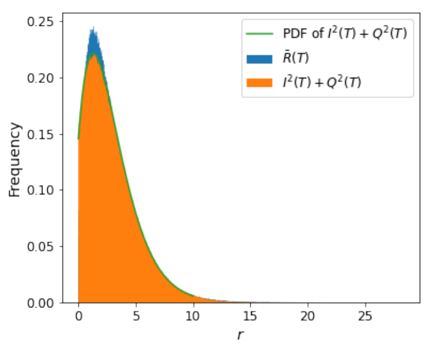

Fig. 6: Rice Fading: Histogram of $\bar{R}(T)$ and $I(T)^2 + Q(T)^2$ using 10^6 samples with the following parameters: $T = 4$, $N = 100$, $I_0 = 0$, $Q_0 = 0$, $k = 1$, $\theta = 1$, and $\beta = 1$.

D. Hoyt Case

Another commonly employed statistical distribution for modeling wireless channels is the Hoyt distribution (also known as the Nakagami-q distribution) [39]. This distribution corresponds to the case in which the in-phase and quadrature are independent jointly Gaussian RVs with a zero mean and different variances. In this case, the processes $I(s)$ and $Q(s)$ satisfy the SDE in (3), where $\theta_1 = \theta_2 = 0$. By applying Ito's formula to derive the non-Markovian SDE for $R(s)$ and subsequently performing the MP, we can determine the drift and diffusion of the projected SDE in (33) as follows:

$$\begin{aligned}\bar{a}(s,r) = &-2k_1 \, \mathbb{E}\left[I^2(s) \mid R(s) = r, I(0) = I_0, Q(0) = Q_0\right] + \beta_1^2 \\ &- 2k_2 \, \mathbb{E}\left[Q^2(s) \mid R(s) = r, I(0) = I_0, Q(0) = Q_0\right] + \beta_2^2,\end{aligned} \tag{54}$$

$$\begin{aligned}\bar{b}^2(s,r) = &\,4\beta_1^2 \mathbb{E}\left[I^2(s) \mid R(s) = r, I(0) = I_0, Q(0) = Q_0\right] \\ &+ 4\beta_2^2 \mathbb{E}\left[Q^2(s) \mid R(s) = r, I(0) = I_0, Q(0) = Q_0\right].\end{aligned} \tag{55}$$

We assume that $I_0 = Q_0 = 0$; consequently, $I(s)$ and $Q(s)$ are zero-mean Gaussian distributions with the following variances:

$$\sigma_1^2(s) = \frac{\beta_1^2}{2k_1}\left(1 - e^{-2k_1 s}\right), \quad \sigma_2^2(s) = \frac{\beta_2^2}{2k_2}\left(1 - e^{-2k_2 s}\right). \tag{56}$$

To compute the conditional expectation in (54) and (55), we must determine $f_{I^2(s)|R(s)}(\cdot \mid \cdot)$, which is expressed as in Proposition 2.

Proposition 2. *If $(I(s), Q(s))$ solves (3) with $\theta_1 = \theta_2 = 0$, $R(s) = I^2(s) + Q^2(s)$, and $I_0 = Q_0 = 0$, then, for $r \geq x$,*

$$f_{I^2(s)|R(s)}(x \mid r) = \frac{(r-x)^{-\frac{1}{2}} \exp\left(-\frac{r-x}{2\sigma_2^2(s)} - \frac{x}{2\sigma_1^2(s)}\right) x^{-\frac{1}{2}}}{\pi \exp\left(-\frac{r(\sigma_1^2(s)+\sigma_2^2(s))}{4\sigma_1^2(s)\sigma_2^2(s)}\right) \mathcal{I}_0\left(\frac{r(\sigma_1^2(s)-\sigma_2^2(s))}{4\sigma_1^2(s)\sigma_2^2(s)}\right)}. \tag{57}$$

Proof: See Appendix C. ∎

Finally, we can compute the conditional expectation $\mathbb{E}\left[I^2(s) \mid R(s) = r\right]$ as follows:

$$\mathbb{E}\left[I^2(s) \mid R(s) = r\right] = \int x f_{I^2(s)|R(s)}(x \mid r) dx. \tag{58}$$

Via the computation, we demonstrate that the simplified expression is given by

$$\begin{aligned}&\mathbb{E}\left[I^2(s) \mid R(s) = r, I(0) = I_0, Q(0) = Q_0\right] \\ &= \frac{r}{2}\left(1 + \frac{\mathcal{I}_1\left(\frac{r}{4}\left(\frac{1}{\sigma_2^2(s)} - \frac{1}{\sigma_1^2(s)}\right)\right)}{\mathcal{I}_0\left(\frac{r}{4}\left(\frac{1}{\sigma_2^2(s)} - \frac{1}{\sigma_1^2(s)}\right)\right)}\right).\end{aligned} \tag{59}$$

Similarly, we can express

$$\begin{aligned}&\mathbb{E}\left[Q^2(s) \mid R(s) = r, I(0) = I_0, Q(0) = Q_0\right] \\ &= \frac{r}{2}\left(1 + \frac{\mathcal{I}_1\left(\frac{r}{4}\left(\frac{1}{\sigma_1^2(s)} - \frac{1}{\sigma_2^2(s)}\right)\right)}{\mathcal{I}_0\left(\frac{r}{4}\left(\frac{1}{\sigma_1^2(s)} - \frac{1}{\sigma_2^2(s)}\right)\right)}\right).\end{aligned} \tag{60}$$

Hence, we have explicit expressions for the drift $\bar{a}(s,r)$ and diffusion $\bar{b}(s,r)$ in the Hoyt case. By using them, we can solve the projected SDE in (33), plot the histogram of the corresponding samples of $\bar{R}(T)$, and compare them to the samples of $I^2(T)+Q^2(T)$, obtained from the original SDE in (3). The results illustrated in Fig. 7 indicate that the MP is an appropriate tool to determine an SDE for the square envelope.

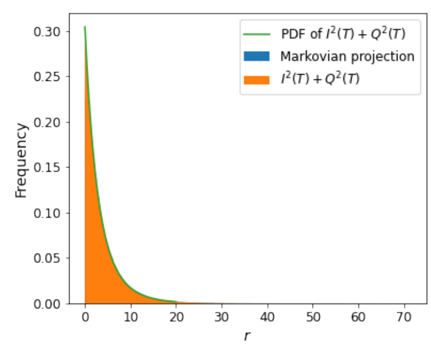

Fig. 7: Hoyt Fading: Histogram of $\bar{R}(T)$ and $I(T)^2 + Q(T)^2$ using 10^6 samples with the following parameters: $T = 4$, $N = 100$, $I_0 = 0$, $Q_0 = 0$, $k_1 = 0.1$, $k_2 = 0.5$, $\beta_1 = \beta_2 = 1$.

V. Numerical Results

A. Monte Carlo

This section provides numerical results for estimating the CCDF of the fade duration, denoted as $Z(T)$, in the context of Rayleigh, Rice, and Hoyt fading. We let $I(s)$ and $Q(s)$ solve (3), and let $\bar{R}(s)$ be the MP of $R(s) = I^2(s) + Q^2(s)$ solving (33). Initially, we employed the MC method to compare the CCDF of $Z(T) = \int_0^T \mathbb{1}_{\{I^2(s)+Q^2(s)<\gamma^2\}} ds$ with the CCDF of

$\bar{Z}(T) = \int_0^T \mathbb{1}_{\{\bar{R}(s)<\gamma^2\}} ds$, aiming to check the effectiveness of working with the lower-dimensional SDE in (33) instead of the original SDE (3). More precisely, the samples of $Z(T)$ are obtained by solving the SDE (6), while the samples of $\bar{Z}(T)$ are obtained by solving the following projected SDE:

$$\begin{cases} \mathrm{d}\bar{R}(s) &= \bar{a}(s, \bar{R})\mathrm{d}s + \bar{b}(s, \bar{R})\mathrm{d}W(s), \\ d\bar{Z}(s) &= \bar{c}(\bar{R}(s))ds, \quad 0 < s < T, \\ \bar{R}(0) &= I_0^2 + Q_0^2, \\ \bar{Z}(0) &= 0, \end{cases} \tag{61}$$

where $\bar{c}(x) = \mathbb{1}_{\{x<\gamma^2\}}$. The projected SDE in (61) is obtained using the MP Lemma 1, by taking $X = (I, Q, I^2 + Q^2, Z)^T$, $P^T = \left(P_1^T, P_2^T\right)$, $P_1 = (0, 0, 1, 0)$, $P_2 = (0, 0, 0, 1)$ and $S = (I^2+Q^2, Z)^T$. We conducted this comparative analysis across various parameter settings in the three fading cases. The results for the Rayleigh, Rice, and Hoyt cases are presented in Figs. 8, 9, and 10, respectively.

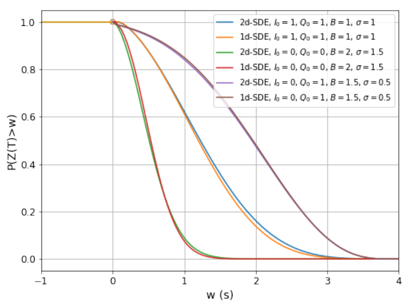

Fig. 8: Estimated complementary cumulative distribution function (CCDF) in the Rayleigh case using the Monte Carlo (MC) method with the following parameters: $T = 4$, $N = 100$, $\gamma = 0.5$, and $M = 10^6$..

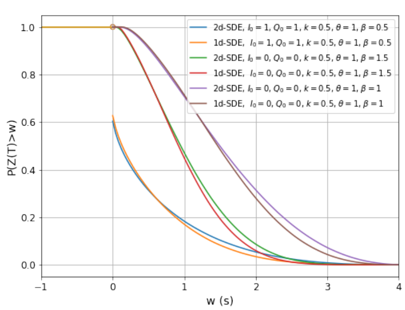

Fig. 9: Estimated complementary cumulative distribution function (CCDF) in the Rice case using the Monte Carlo (MC) method with the following parameters: $T = 4$, $N = 100$, $\gamma = 1$, and $M = 10^6$.

The remarkable consistency observed across all cases suggests that using the projected process $\bar{R}$ instead of (I, Q), does not noticeably change the CCDF of the fade duration. The discrepancy between the CCDFs of $Z(T)$ and $\bar{Z}(T)$ in the Rice case stems from using the approximated drift $\tilde{a}$ instead of the precise drift a. In contrast, for the Rayleigh and Hoyt cases, we employed exact expressions for drift and diffusion. Consequently, the divergence between the CCDFs primarily arises from discretization errors. Significantly, an augmented number of time steps N results in a more accurate fitting of the curves.

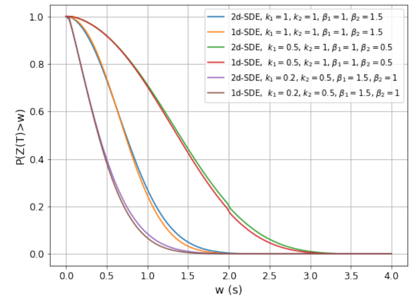

Fig. 10: Estimated complementary cumulative distribution function (CCDF) in the Hoyt case using the Monte Carlo (MC) method with the following parameters: $T = 4$, $N = 200$, $\gamma = 0.5$, and $M = 10^6$.

In the next experiment, we employed the MC method to examine how the distribution of the fade duration $Z(T)$ behaves when we manipulate the parameters of the channel. Specifically, in the Rayleigh case, the parameters B and σ exert control over the autocorrelation of the complex envelope $I + iQ$. Notably, $I(t)$ and $Q(t)$ are independent; thus, we can express the autocorrelation of the complex envelop as $C_{II}(\Delta t) + C_{QQ}(\Delta t) \overset{T\to\infty}{=} \sigma^2 e^{-\frac{1}{2}B\Delta t}$. Consequently, B represents the correlation time scale, and the autocorrelation of the signal increases linearly with σ^2.

Fig. 11 presents a comparative analysis of the behavior of the estimated CCDF of $Z(T)$ in the Rayleigh case by solving (6), as we manipulated the parameters B and σ. Altering the parameter B has a relatively minor effect on the shape of the CCDF and the associated calculated statistics. In contrast, when the parameter σ is adjusted, even a slight modification can result in a significant transformation in the distribution of $Z(T)$. Furthermore, the results demonstrate that as both B and σ increase, the CCDF experiences a more rapid decay towards zero. Additionally, as B increases and σ decreases, the probability $P(Z(T) = 0)$ tends toward zero, signifying that the RV $Z(T)$ transitions towards a continuous distribution when the signal exhibits lower levels of correlation.

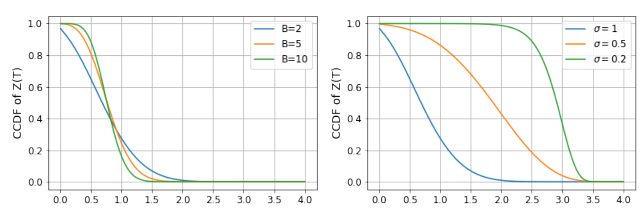

(a) $\sigma = 1$ (b) $B = 2$

Fig. 11: Estimated complementary cumulative distribution function (CCDF) using the Monte Carlo (MC) method, for various values of B and σ with the following fixed parameters: $T = 4$, $N = 100$, $I_0 = 1$, $Q_0 = 1$, $\gamma = 0.5$, and $M = 10^6$.

Another noteworthy experiment involves keeping the channel parameters fixed while varying the threshold γ. Fig. 12 presents the variations of the CCDF of $Z(T)$. The observations indicate that as the threshold rises, the CCDF of $Z(T)$ undergoes a more rapid decay toward zero, and the magnitude of the jump at zero diminishes.

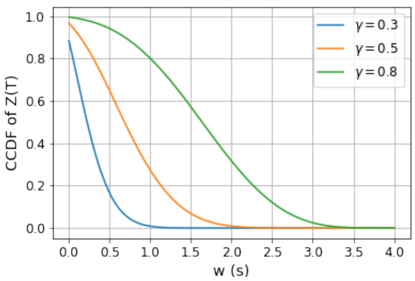

Fig. 12: Estimated complementary cumulative distribution function (CCDF) using Monte Carlo (MC) method, for various values of γ with the following parameters: $T = 4$, $N = 100$, $I_0 = 1$, $Q_0 = 1$, $B = 2$, and $\sigma = 1$.

B. Importance Sampling

This section presents the numerical results for the IS estimator employed in the right-tail estimation of the CCDF of fade duration in the Rayleigh and Rice cases. We follow the methodology outlined in Section III-B to determine an appropriate change of measure and reduce the variance of the proposed estimator. Obtaining the optimal change of measure entails solving the KBE in (28). As discussed in Remark 2, to circumvent the challenges posed by the curse of dimensionality, it is crucial to apply the change of measure to the projected SDE in (61).

In the Rayleigh case, we have derived the exact drift and diffusion terms of the projected SDE (61). This guarantees that the conditional distributions of $(\bar{R}, \bar{Z})$ and (R, Z) are the same, leading to $\mathbb{E}[g_w(Z(T)) \mid I(t) = I_t, Q(t) = Q_t, Z(t) = z] = \mathbb{E}[g_w(\bar{Z}(T)) \mid I(t) = I_t, Q(t) = Q_t, \bar{Z}(t) = z]$. Consequently, we can solve the SDE (61) instead of the full-dimensional SDE (6) and apply the change of measure to the projected SDE without introducing any bias.

However, in the Rice case, where the exact expressions for drift and diffusion cannot be determined, applying the same strategy as in the Rayleigh case may lead to bias if we solve the SDE (61) with an approximated drift. To mitigate this bias, our approach involves solving the KBE for the projected SDE, and then mapping the projected control from the reduced-dimension SDE back to the full-dimensional SDE. This method ensures the elimination of bias, as IS is applied to the original full dimensional SDE. Further details will be provided in Section V-B2.

1) Rayleigh Fading: We applied the optimal change of measure on the projected SDE in (61), where the drift $\bar{a}(s,r)$ is determined by (35) and the diffusion $\bar{b}(s,r)$ is specified by (36). The modified processes $(\bar{R}_{\zeta^*}, \bar{Z}_{\zeta^*})$ satisfy the following controlled SDE:

$$\begin{cases} d\bar{R}_{\zeta^*}(s) = B\left(\sigma^2 - \bar{R}_{\zeta^*}(s)\right) ds \\ +\sigma\sqrt{2B\bar{R}_{\zeta^*}(s)}\, \zeta^*(s, \bar{R}_{\zeta^*}(s), \bar{Z}_{\zeta^*}(s)) ds + \sigma\sqrt{2B\bar{R}_{\zeta^*}(s)} dW(s), \\ d\bar{Z}_{\zeta^*}(s) = \bar{c}(\bar{R}_{\zeta^*}(s)) ds, \quad 0 < s < T, \\ \bar{R}_{\zeta^*}(0) = \bar{R}(0), \\ \bar{Z}_{\zeta^*}(0) = \bar{Z}(0), \end{cases} \tag{62}$$

where the optimal control is defined as

$$\zeta^*(t,x,z) = \sigma\sqrt{2Bx}\, \partial_x \log v(t,x,z), \tag{63}$$

and $v(t,x,z) = \mathbb{E}[g_w(\bar{Z}(T)) \mid \bar{R}(t) = x, \bar{Z}(t) = z]$ is the solution of the following PDE, for $x \geq 0,\ 0 \leq t \leq T$, and $t - (T - w) \leq z \leq t$,

$$\begin{cases} \partial_t v(t,x,z) + B\left(\sigma^2 - x\right)\partial_x v(t,x,z) + \bar{c}(z)\partial_z v(t,x,z) \\ \quad + \sigma^2 B x \partial_{xx} v(t,x,z) = 0, \\ v(T,x,z) = g_w(z), \quad \text{(+ Boundary conditions)}. \end{cases} \tag{64}$$

The optimal IS estimator is given by

$$\mathcal{A}_{IS^*} = \frac{1}{M_{IS}} \sum_{k=1}^{M_{IS}} g_w\left(\bar{Z}_{\zeta^*}^{(k)}(T)\right) \exp\left\{ -\int_t^T \frac{1}{2}\zeta^{*2}\left(s, \bar{R}_{\zeta^*}^{(k)}(s), \bar{Z}_{\zeta^*}^{(k)}(s)\right) \mathrm{d}s - \int_t^T \zeta^*\left(s, \bar{R}_{\zeta^*}^{(k)}(s), \bar{Z}_{\zeta^*}^{(k)}(s)\right) \mathrm{d}W(s)\right\}, \tag{65}$$

where M_{IS} is the number of samples for the IS estimator. Moreover, the relative error of the IS estimator can be expressed as follows

$$\epsilon_{IS} = C\frac{\sqrt{\mathrm{Var}\left[\mathcal{A}_{IS^*}\right]}}{\sqrt{M_{IS}}P(\bar{Z}(T) > w)}. \tag{66}$$

It is important to note that our proposed estimator is unbiased, as we use the exact drift and diffusion terms of the projected SDE in the Rayleigh case, and both the original and projected SDEs have the same initial condition. To verify the unbiasedness of the IS estimator, we generated Fig. 13, which shows the estimated CCDF for values of w greater than two, along with the corresponding relative error.

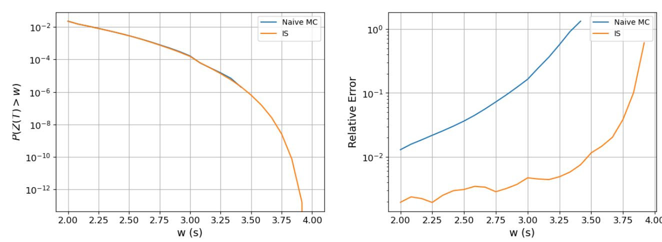

Fig. 13: Estimated tail of the complementary cumulative distribution function (CCDF) and the corresponding relative error using the Monte Carlo (MC) and importance sampling (IS) methods in the Rayleigh case with the following parameters: $T = 4$, $N = 100$, $I_0 = 1$, $Q_0 = 1$, $B = 1$, $\sigma = 1$, $\gamma = 0.5$, and $M_{MC} = M_{IS} = 10^6$.

We observed consistency in the estimation of the CCDF using the MC and IS methods for $w < 3.5$. The MC estimator estimates $P(Z(T) > w)$ as zero for $w \geq 3.5$ but exhibits a remarkably high relative error. Conversely, the IS estimator approximates the right tail of the CCDF at minimal values with a reasonable relative error. Fig. 14 presents the number of samples needed to achieve a 5% relative error using the IS and MC methods. A substantial amount of variance reduction occurs when using IS compared to the crude MC method.

For a better view of the results, Table I presents the estimated value of $P(Z(T) > w)$ and corresponding variance for various values of w, using both estimators. We employed 10^6 samples for the MC and IS estimators across the entire range for w. Table I reveals that the optimal IS estimator effectively estimates very small values, as low as 10^{-9}, with a relative error below 5%. In addition, it estimates $P(Z(T) > 3.83)$ as 7.5×10^{-11} with only a 10% relative error.

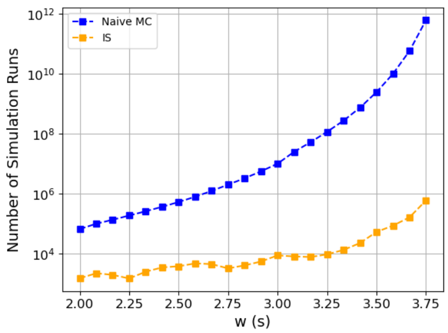

Fig. 14: Number of required simulation runs for a 5% relative error for the projected process, using the importance sampling (IS) and naive Monte Carlo (MC) methods, in the Rayleigh case with the following parameters: $T = 4$, $N = 100$, $I_0 = 1$, $Q_0 = 1$, $B = 1$, $\sigma = 1$, and $\gamma = 0.5$.

w	$\mathcal{A}_{MC}$	$\mathcal{A}_{IS^*}$	$Var[\mathcal{A}_{MC}]$	$Var[\mathcal{A}_{IS^*}]$
2.5	0.003	0.0028	0.0034	2.09×10^{-5}
3	1.8×10^{-4}	1.5×10^{-4}	1.8×10^{-4}	1.16×10^{-7}
3.25	1.7×10^{-5}	1.34×10^{-5}	1.7×10^{-5}	1.11×10^{-9}
3.5	0	6.048×10^{-7}		1.41×10^{-11}
3.75	0	2.58×10^{-9}		2.59×10^{-15}
3.83	0	7.5×10^{-11}		1.51×10^{-17}

TABLE I: Comparison of the Monte Carlo (MC) and importance sampling (IS) estimators for values of w with the following parameters: $N = 100$, $I_0 = 1$, $Q_0 = 1$, $B = 1$, $\sigma = 1$, and $\gamma = 0.5$.

2) Rice Fading: In this case, we do not have the exact expression for the drift of the projected SDE (33); instead, we only have the approximated drift $\tilde{a}(s, r)$, as given by (53). If we use this approximation to solve the projected SDE, it will introduce bias in estimating $\mathbb{E}[g_w(\bar{Z}(T)) \mid I(t) = I_t, Q(t) = Q_t, \bar{Z}(t) = z]$ relative to $\mathbb{E}[g_w(Z(T)) \mid I(t) = I_t, Q(t) = Q_t, Z(t) = z]$. To avoid this bias, we apply a change of measure to the original SDE (6). The controlled processes $(I_\zeta, Q_\zeta, Z_\zeta)$ then solve the following controlled SDE:

$$\begin{cases} dI_\zeta(s) = \Big(k\big(\theta - I_\zeta(s)\big) + \beta\ \zeta_1(s, I_\zeta(s), Q_\zeta(s), Z_\zeta(s))\Big)ds \\ \qquad\qquad + \beta dW^{(I)}(s), \\ dQ_\zeta(s) = \Big(k\big(\theta - Q_\zeta(s)\big) + \beta\ \zeta_2(s, I_\zeta(s), Q_\zeta(s), Z_\zeta(s))\Big)ds \\ \qquad\qquad + \beta dW^{(Q)}(s), \\ dZ_\zeta(s) = f(I_\zeta(s), Q_\zeta(s))ds, \quad 0 < s < T, \\ I_\zeta(0) = I_0, \\ Q_\zeta(0) = Q_0, \\ Z_\zeta(0) = 0, \end{cases} \tag{67}$$

where ζ_1, ζ_2 represent the controls.

Obtaining an optimal control requires solving a high-dimensional PDE, as discussed in Remark 2. As an alternative, we propose suboptimal controls by utilizing the optimal change of measure for the projected SDE and mapping it to the full-dimensional SDE. Specifically, the optimal controls (ζ_1^*, ζ_2^*) for the full-dimensional SDE under the optimal change of measure can be expressed as:

$$\begin{aligned} \zeta_1^*(t, x, y, z) &= \beta\ \partial_x \log v_H(t, x, y, z), \\ \zeta_2^*(t, x, y, z) &= \beta\ \partial_y \log v_H(t, x, y, z), \end{aligned} \tag{68}$$

where $v_H(t, x, y, z)$ is the solution to the KBE (28) associated with the SDE (6). However, solving this KBE is computationally expensive. Alternatively, we approximate $v_H(t, x, y, z)$ by $v_L(t, x^2 + y^2, z)$, where $v_L(t, r, z)$ is the solution to the KBE of the projected SDE (61), with approximated drift $\tilde{a}(s, r)$ and diffusion given by (43). The function $v_L(t, r, z)$ is therefore the solution to the following PDE, for $r \geq 0$, $0 \leq t \leq T$, and $t - (T - w) \leq z \leq t$:

$$\begin{cases} \partial_t v_L(t, r, z) + \tilde{a}(s, r)\partial_r v_L(t, r, z) + \bar{c}(z)\partial_z v(t, x, z) \\ \quad + 2\beta^2 r \partial_{rr} v_L(t, r, z) = 0, \\ v_L(T, r, z) = g_w(z), \quad \text{(+ Boundary conditions).} \end{cases} \tag{69}$$

Finally, the suboptimal controls ζ_1 and ζ_2 are given by:

$$\begin{aligned} \zeta_1(t, x, y, z) &= 2\beta\ x\ \frac{\partial_r v_L(t, x^2 + y^2, z)}{v_L(t, x^2 + y^2, z)}, \\ \zeta_2(t, x, y, z) &= 2\beta\ y\ \frac{\partial_r v_L(t, x^2 + y^2, z)}{v_L(t, x^2 + y^2, z)}. \end{aligned} \tag{70}$$

The IS estimator is given by:

$$\begin{aligned} \mathcal{A}_{IS} = \frac{1}{M_{IS}} \sum_{k=1}^{M_{IS}} & g_w\left(Z_\zeta^{(k)}(T)\right) \\ & \exp\Big\{ - \int_t^T \frac{1}{2}{\zeta_1}^2 \left(s, I_\zeta^{(k)}(s), Q_\zeta^{(k)}(s), Z_\zeta^{(k)}(s)\right) ds \\ & - \int_t^T \frac{1}{2}{\zeta_2}^2 \left(s, I_\zeta^{(k)}(s), Q_\zeta^{(k)}(s), Z_\zeta^{(k)}(s)\right)\ \mathrm{d}s \\ & - \int_t^T \zeta_1 \left(s, I_\zeta^{(k)}(s), Q_\zeta^{(k)}(s), Z_\zeta^{(k)}(s)\right)\ \mathrm{d}W^{(I)}(s) \\ & - \int_t^T \zeta_2 \left(s, I_\zeta^{(k)}(s), Q_\zeta^{(k)}(s), Z_\zeta^{(k)}(s)\right)\ \mathrm{d}W^{(Q)}(s) \Big\}. \end{aligned} \tag{71}$$

In Fig.15, we plot the estimated CCDF for w values greater than two using both the MC and IS estimators. The results confirm that the proposed IS estimator is unbiased.

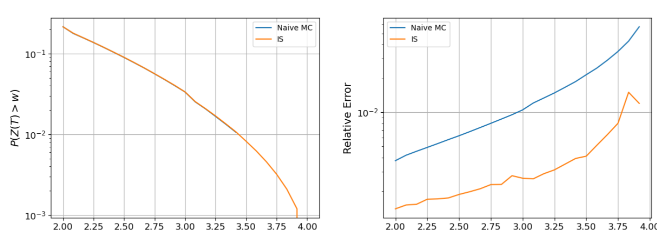

Fig. 15: Estimated tail of the complementary cumulative distribution function (CCDF) and the corresponding relative error using the Monte Carlo (MC) and importance sampling (IS) methods in the Rice case with the following parameters: $T = 4$, $N = 100$, $I_0 = 0$, $Q_0 = 0$, $\theta = 1$, $k = 1$, $\beta = 1$, $\gamma = 0.5$, and $M_{MC} = M_{IS} = 10^6$.

Additionally, Fig.16 shows the number of samples required to achieve a 5% relative error using the IS and MC methods. The IS method reduced the number of simulation runs by about 20 times, compared to the MC estimator, for $w \geq 3$. This demonstrates the effectiveness of the proposed suboptimal change of measure in achieving variance reduction.

This article has been accepted for publication in IEEE Transactions on Wireless Communications. This is the author's version which has not been fully edited and content may change prior to final publication. Citation information: DOI 10.1109/TWC.2025.3536615

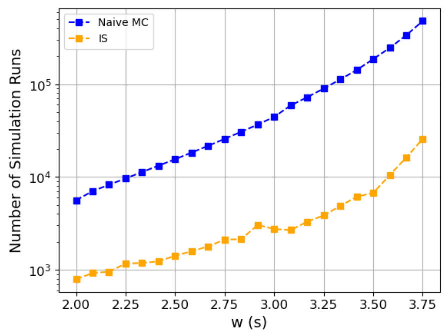

Fig. 16: Number of required simulation runs for a 5% relative error using the importance sampling (IS) and naive Monte Carlo (MC) methods, in the Rice case with the following parameters: $T = 4$, $N = 100$, $I_0 = 0$, $Q_0 = 0$, $\theta = 1$, $k = 1$, $\beta = 1$, $\gamma = 0.5$, and $M = M_{IS} = 10^6$.

VI. Conclusion

This work developed more realistic stochastic models to represent time-varying wireless channels, using SDEs and MP to investigate channel envelope dynamics across various fading scenarios. The results for the Rayleigh case align with those developed using a different method in [29]. Furthermore, we extended this analysis to derive SDEs for more general cases, including the Rice and Hoyt envelopes.

The paper also focused on the performance analysis of stochastic channels. Notably, we introduced the fading duration metric, which measures the time during which the channel remains faded (i.e., below a given threshold). Using the dynamical models derived in the first part, we estimated the CCDF of this duration in the Rayleigh, Rice, and Hoyt cases. We employed the MC method on the original and projected SDEs and demonstrated the consistency of the results, verifying the effectiveness of using MP. Additionally, we explored how the CCDF behaves when altering the signal autocorrelation parameters.

Finally, we used IS to estimate the tail of the CCDF accurately. We proposed an optimal change of measure for the Rayleigh case and a suboptimal optimal change of measure in the Rice case, highlighting significant gains in terms of variance reduction, yielding more precise tail estimations.

Appendix A
Statistics of $I(T)$, $Q(T)$ and $\bar{R}(T)$

From the SDE in (3), the expression of $I(T)$ can be written as follows:

$$I(T) = I_t\, e^{-k_1(T-t)} + \theta_1\left(1 - e^{-k_1(T-t)}\right) + \beta_1 \int_t^T e^{-k(T-u)} dW(u) \tag{72}$$

Therefore, the statistics of $I(T)$ (and similarly $Q(T)$) are given by

$$E\left[I(T)\right] = I_t\, e^{-k_1(T-t)} + \theta_1\left(1 - e^{-k_1(T-t)}\right) \xrightarrow{T\to\infty} \theta_1$$
$$Var\left[I(T)\right] = \frac{\beta_1^2}{2k_1}\left(1 - e^{-2k_1(T-t)}\right) \xrightarrow{T\to\infty} \frac{\beta_1^2}{2k_1}, \tag{73}$$

$$\begin{aligned}
&C_{II}(s, s+\Delta s)\\
&= E\left[\beta_1^2 \int_t^s e^{-k_1(s-u)} dW(u) \int_t^{s+\Delta s} e^{-k_1(s+\Delta s-u)} dW(u)\right]\\
&= \beta_1^2 e^{-k_1 s} e^{-k_1(s+\Delta s)} E\left[\int_t^s e^{k_1 u} dW(u) \int_t^{s+\Delta s} e^{k_1 u} dW(u)\right]\\
&= \beta_1^2 e^{-2k_1 s - k_1\Delta s} \int_t^s e^{2k_1 u} du\\
&= \frac{\beta_1^2}{2k_1} e^{-k_1\Delta s}\left(1 - e^{-2k_1 s}\right) \xrightarrow{s\to\infty} \frac{\beta_1^2}{2k_1} e^{-k_1\Delta s}.
\end{aligned} \tag{74}$$

By solving the SDE in (37), we have

$$\begin{aligned}
&d\bar{R}(s) = B\left(\sigma^2 - \bar{R}(s)\right) ds + \sigma\sqrt{2B\bar{R}(s)}\, dW(s)\\
&e^{Bs} d\bar{R}(s) + Be^{Bs}\bar{R}(s) ds = B\sigma^2 e^{Bs} ds + \sigma\sqrt{2B\bar{R}(s)}\, e^{Bs} dW(s)\\
&d\left(e^{Bs}\bar{R}(s)\right) = B\sigma^2 e^{Bs} ds + \sigma\sqrt{2B\bar{R}(s)}\, e^{Bs} dW(s)\\
&e^{BT}\bar{R}(T) - \bar{R}(0) = B\sigma^2 \int_0^T e^{Bs} ds + \sigma \int_0^T \sqrt{2B\bar{R}(s)}\, e^{Bs} dW(s)\\
&= \sigma^2\left(e^{BT} - 1\right) + \sigma \int_0^T \sqrt{2B\bar{R}(s)}\, e^{Bs} dW(s).
\end{aligned} \tag{75}$$

Using the properties of Ito integrals, we can write the expectation, the variance, and the autocorrelation of $\bar{R}(T)$ as follows:

$$E[\bar{R}(T)] = e^{-BT}\bar{R}(0) + \sigma^2\left(1 - e^{-BT}\right) \xrightarrow{T\to\infty} \sigma^2 \tag{76}$$

$$\begin{aligned}
&\mathrm{Var}(\bar{R}(T)) = \sigma^2 E\left[\left(\int_0^T \sqrt{2B\bar{R}(s)}\, e^{-B(T-s)} dW(s)\right)^2\right]\\
&= \sigma^2 \int_0^T E\left[2B\bar{R}(s) e^{-2B(T-s)}\right] ds\\
&= 2B\sigma^2 e^{-2BT} \int_0^T \left[e^{-Bs}\bar{R}(0) + \sigma^2\left(1 - e^{-Bs}\right)\right] e^{2Bs} ds\\
&= \sigma^2\left[2\left(\bar{R}(0) - \sigma^2\right)\left(e^{-BT} - e^{-2BT}\right) + \sigma^2\left(1 - e^{-2BT}\right)\right]\\
&\xrightarrow{T\to\infty} \sigma^4
\end{aligned} \tag{77}$$

$$\begin{aligned}
C_{\bar{R}\bar{R}}(t, t+\Delta t) &= \sigma^2 \mathbb{E}\left[\int_0^t \sqrt{2B\bar{R}(s)}\, e^{-B(t-s)} dW(s)\right.\\
&\qquad \left.\int_0^{t+\Delta t} \sqrt{2B\bar{R}\,(s)}\, e^{-B(t+\Delta t-s)} dW(s)\right]\\
&= \sigma^2 \int_0^t \mathbb{E}[2B\bar{R}(s)] e^{-2B(t-s)} e^{-B\Delta t} ds\\
&= 2B\sigma^2 e^{-2Bt} e^{-B\Delta t} \int_0^t e^{Bs}\bar{R}(0) + \sigma^2\left(1 - e^{-Bs}\right) e^{2Bs} ds\\
&= \sigma^2 e^{-B\Delta t}\left(2\left(\bar{R}(0) - \sigma^2\right)\left(e^{-Bt} - e^{-2Bt}\right) + \sigma^2\left(1 - e^{-2Bt}\right)\right)\\
&\xrightarrow{t\to\infty} \sigma^4 e^{-B\Delta t}.
\end{aligned} \tag{78}$$

Appendix B
Proof of Proposition 1

We write the conditional PDF $f_{I(s)|R(s)}(x \mid r)$ for $r > x^2$ as follows:

$$f_{I(s)|R(s)}(x \mid r) = \frac{f_{I(s)R(s)}(x,r)}{f_{R(s)}(r)} = \frac{f_{R(s)|I(s)}(x,r) f_{I(s)}(x)}{f_{R(s)}(r)}. \tag{79}$$

First, we know that $\sqrt{R(s)}$ has a Rice distribution with parameters $(\sqrt{2}m(s), \sigma(s))$. The PDF of $\sqrt{R(s)}$, for $x \geq 0$, is given by

$$f_{\sqrt{R(s)}}(x) = \frac{x}{\sigma^2(s)} \exp\left(-\frac{2m^2(s)+x^2}{2\sigma^2(s)}\right) \mathcal{I}_0\left(\frac{x\sqrt{2}m(s)}{\sigma^2(s)}\right). \tag{80}$$

Therefore, for $r \geq 0$,

$$\begin{aligned} f_{R(s)}(r) &= \frac{1}{2\sqrt{r}} f_{\sqrt{R(s)}}(\sqrt{r}) \\ &= \frac{1}{2\sigma^2(s)} \exp\left(-\frac{2m^2(s)+r}{2\sigma^2(s)}\right) \mathcal{I}_0\left(\frac{m(s)\sqrt{2r}}{\sigma^2(s)}\right). \end{aligned} \tag{81}$$

In contrast,

$$f_{R(s)|I(s)}(r \mid x) = f_{I^2(s)+Q^2(s)|I(s)=x}(r) = f_{Q^2(s)}(r-x^2) \tag{82}$$

We know that $\frac{Q^2(s)}{\sigma^2(s)}$ has a noncentral chi-square distribution with one degree of freedom and the parameter $\lambda(s) = \frac{m^2(s)}{\sigma^2(s)}$. Therefore, for $r > x^2$,

$$\begin{aligned} & f_{R(s)|I(s)}(r \mid x) \\ &= \frac{1}{2\sigma^2(s)} \exp\left(-\frac{r-x^2}{2\sigma^2(s)} - \frac{\lambda(s)}{2}\right) \left(\frac{r-x^2}{\lambda(s)\sigma^2(s)}\right)^{-\frac{1}{4}} \\ &\times \mathcal{I}_{-\frac{1}{2}}\left(\frac{\sqrt{\lambda(s)(r-x^2)}}{\sigma(s)}\right). \end{aligned} \tag{83}$$

Finally, for $r > x^2$, we obtain

$$f_{I(s)|R(s)}(x \mid r) = \frac{\exp\left(\frac{xm(s)}{\sigma^2(s)}\right)\left(\frac{r-x^2}{m^2(s)}\right)^{-\frac{1}{4}} \mathcal{I}_{-\frac{1}{2}}\left(\frac{m(s)\sqrt{(r-x^2)}}{\sigma^2(s)}\right)}{\sqrt{2\pi}\sigma(s)\mathcal{I}_0\left(\frac{m(s)\sqrt{2r}}{\sigma^2(s)}\right)}. \tag{84}$$

Appendix C
Proof of Proposition 2

We write the conditional PDF $f_{I^2(s)|R(s)}(x \mid r)$ for $r \geq x$ as follows:

$$f_{I^2(s)|R(s)}(x \mid r) = \frac{f_{I^2(s)R(s)}(x,r)}{f_{R(s)}(r)} = \frac{f_{R(s)|I^2(s)}(x,r) f_{I^2(s)}(x)}{f_R(r)}. \tag{85}$$

Additionally, $R(s)$ has a square Hoyt distribution, and its PDF can be written as follows [39]:

$$\begin{aligned} f_{R(s)}(r) &= \frac{1}{2\sigma_1(s)\sigma_2(s)} \exp\left(-\frac{r(\sigma_1^2(s)+\sigma_2^2(s))}{4\sigma_1^2(s)\sigma_2^2(s)}\right) \\ &\times \mathcal{I}_0\left(\frac{r(\sigma_1^2(s)-\sigma_2^2(s))}{4\sigma_1^2(s)\sigma_2^2(s)}\right),\ r \geq 0. \end{aligned} \tag{86}$$

We can express $f_{R(s)|I^2(s)}(x,r)$ and $f_{I^2(s)}(x)$ as follows because $\frac{I^2(s)}{\sigma_1^2(s)}$ and $\frac{Q^2(s)}{\sigma_2^2(s)}$ follow chi-squared distributions with one degree of freedom:

$$f_{R(s)|I^2(s)}(x,r) = \frac{1}{\sqrt{2\pi\sigma_2^2(s)}}\left(\frac{r-x}{\sigma_2^2(s)}\right)^{-\frac{1}{2}} \exp\left(-\frac{r-x}{2\sigma_2^2(s)}\right), \tag{87}$$

and

$$f_{I^2(s)}(x) = \frac{1}{\sqrt{2\pi\sigma_1^2(s)}}\left(\frac{x}{\sigma_1^2(s)}\right)^{-\frac{1}{2}} \exp\left(-\frac{x}{2\sigma_1^2(s)}\right). \tag{88}$$

Substituting (86), (87), and (88) into (85), we obtain:

$$f_{I^2(s)|R(s)}(x \mid r) = \frac{(r-x)^{-\frac{1}{2}} \exp\left(-\frac{r-x}{2\sigma_2^2(s)} - \frac{x}{2\sigma_1^2(s)}\right) x^{-\frac{1}{2}}}{\pi \exp\left(-\frac{r(\sigma_1^2(s)+\sigma_2^2(s))}{4\sigma_1^2(s)\sigma_2^2(s)}\right)\mathcal{I}_0\left(\frac{r(\sigma_1^2(s)-\sigma_2^2(s))}{4\sigma_1^2(s)\sigma_2^2(s)}\right)}. \tag{89}$$

References

[1] L. Zhu, W. Ma, and R. Zhang, "Modeling and performance analysis for movable antenna enabled wireless communications," *IEEE Transactions on Wireless Communications*, 2023.

[2] Y. Bian, D. Dong, J. Jiang, and K. Song, "Performance analysis of reconfigurable intelligent surface-assisted wireless communication systems under co-channel interference," *IEEE Open Journal of the Communications Society*, vol. 4, pp. 596–605, 2023.

[3] S. Iyer, "Performance analysis of a dynamic spectrum assignment technique for 6g," *IETE Journal of Research*, vol. 69, no. 11, pp. 7695–7703, 2023.

[4] Q. Zhang, D.-W. Yue, and X.-Y. Xu, "Performance analysis of reconfigurable intelligent surface-assisted underwater wireless optical communication systems," *IEEE Photonics Journal*, 2024.

[5] S. Dastoor and H. Patel, "Performance analysis of massive mimo using various transmit precoding schemes for a wireless network," *International Journal of Communication Systems*, p. e5785, 2024.

[6] J. Ye, S. Dang, G. Ma, O. Amin, B. Shihada, and M.-S. Alouini, "On outage performance of terahertz wireless communication systems," *IEEE Transactions on Communications*, vol. 70, no. 1, pp. 649–663, 2021.

[7] K. Sowerby and A. Williamson, "Outage probability calculations for multiple cochannel interferers in cellular mobile radio systems," in *IEE Proceedings F (Communications, Radar and Signal Processing)*, vol. 135, no. 3. IET, 1988, pp. 208–215.

[8] A. Abdi, K. Wills, H. A. Barger, M.-S. Alouini, and M. Kaveh, "Comparison of the level crossing rate and average fade duration of rayleigh, rice and nakagami fading models with mobile channel data," in *Vehicular Technology Conference Fall 2000. IEEE VTS Fall VTC2000. 52nd Vehicular Technology Conference (Cat. No. 00CH37152)*, vol. 4. IEEE, 2000, pp. 1850–1857.

[9] X. Dong and N. C. Beaulieu, "Average level crossing rate and average fade duration of selection diversity," *IEEE Communications Letters*, vol. 5, no. 10, pp. 396–398, 2001.

[10] N. C. Beaulieu and X. Dong, "Level crossing rate and average fade duration of mrc and egc diversity in ricean fading," *IEEE transactions on communications*, vol. 51, no. 5, pp. 722–726, 2003.

[11] X. Cheng, C.-X. Wang, B. Ai, and H. Aggoune, "Envelope level crossing rate and average fade duration of nonisotropic vehicle-to-vehicle ricean fading channels," *IEEE transactions on intelligent transportation systems*, vol. 15, no. 1, pp. 62–72, 2013.

[12] N. Zlatanov, Z. Hadzi-Velkov, and G. K. Karagiannidis, "Level crossing rate and average fade duration of the double nakagami-m random process and application in mimo keyhole fading channels," *IEEE Communications Letters*, vol. 12, no. 11, pp. 822–824, 2008.

[13] L. Yang, M. O. Hasna, and M.-S. Alouini, "Average outage duration of multihop communication systems with regenerative relays," *IEEE Transactions on Wireless Communications*, vol. 4, no. 4, pp. 1366–1371, 2005.

[14] C. B. Issaid and M.-S. Alouini, "Level crossing rate and average outage duration of free space optical links," *IEEE Transactions on Communications*, vol. 67, no. 9, pp. 6234–6242, 2019.

[15] C.-X. Wang, Z. Lv, Y. Chen, and H. Haas, "A complete study of space-time-frequency statistical properties of the 6g pervasive channel model," *IEEE Transactions on Communications*, 2023.

[16] S. J. Nawaz, M. Adil, and S. Wyne, "Average contiguous duration-a novel metric for characterizing wireless fading channels," *IEEE Wireless Communications Letters*, vol. 10, no. 8, pp. 1790–1794, 2021.

[17] J.-i. Takada, T. Aoyagi, K. Takizawa, N. Katayama, T. Kobayashi, K. Y. Yazdandoost, H.-b. Li, and R. Kohno, "Static propagation and channel models in body area," in *COST 2100 6th Management Committee Meeting*, 2008.

[18] A. S. Avestimehr, S. N. Diggavi, and N. David, "Wireless network information flow: A deterministic approach," *IEEE Transactions on Information theory*, vol. 57, no. 4, pp. 1872–1905, 2011.

[19] Y.-X. Wang, Z.-Y. Liu, and L.-X. Guo, "Research on mimo channel capacity in complex indoor environment based on deterministic channel model," in *2021 IEEE/CIC International Conference on Communications in China (ICCC Workshops)*. IEEE, 2021, pp. 405–409.

[20] N. Moraitis and D. Vouyioukas, "Indoor deterministic-based channel modeling at d-band for 6g wireless networks," in *2023 IEEE 97th Vehicular Technology Conference (VTC2023-Spring)*. IEEE, 2023, pp. 1–5.

[21] M. M. Olama, K. K. Jaladhi, S. M. Djouadi, C. D. Charalambous *et al.*, "Recursive estimation and identification of time-varying long-term fading channels," *Journal of Electrical and Computer Engineering*, vol. 2007, 2007.

[22] T. Feng and T. R. Field, "Statistical analysis of mobile radio reception: An extension of clarke's model," *IEEE transactions on communications*, vol. 56, no. 12, pp. 2007–2012, 2008.

[23] J. Bian, C.-X. Wang, X. Gao, X. You, and M. Zhang, "A general 3d non-stationary wireless channel model for 5g and beyond," *IEEE Transactions on Wireless Communications*, vol. 20, no. 5, pp. 3211–3224, 2021.

[24] X. Wang, Y. Shi, W. Xin, T. Wang, G. Yang, and Z. Jiang, "Channel prediction with time-varying doppler spectrum in high-mobility scenarios: A polynomial fourier transform based approach and field measurements," *IEEE Transactions on Wireless Communications*, vol. 22, no. 11, pp. 7116–7129, 2023.

[25] T. Feng, T. R. Field, and S. Haykin, "Stochastic differential equation theory applied to wireless channels," *IEEE Transactions on Communications*, vol. 55, no. 8, pp. 1478–1483, 2007.

[26] M. M. Olama, S. M. Djouadi, and C. D. Charalambous, "Stochastic differential equations for modeling, estimation and identification of mobile-to-mobile communication channels," *IEEE Transactions on Wireless Communications*, vol. 8, no. 4, pp. 1754–1763, 2009.

[27] C. D. Charalambous and N. Menemenlis, "A state-space approach in modeling multipath fading channels via stochastic differential equations," in *ICC 2001. IEEE International Conference on Communications. Conference Record (Cat. No. 01CH37240)*, vol. 7. IEEE, 2001, pp. 2251–2255.

[28] C. D. Charalambous, R. J. Bultitude, X. Li, and J. Zhan, "Modeling wireless fading channels via stochastic differential equations: identification and estimation based on noisy measurements," *IEEE Transactions on Wireless Communications*, vol. 7, no. 2, pp. 434–439, 2008.

[29] C. D. Charalambous and N. Menemenlis, "Stochastic models for short-term multipath fading channels: chi-square and ornstein-uhlenbeck processes," in *Proceedings of the 38th IEEE Conference on Decision and Control (Cat. No. 99CH36304)*, vol. 5. IEEE, 1999, pp. 4959–4964.

[30] M. M. Olama, S. M. Djouadi, and C. D. Charalambous, "Stochastic power control for time-varying long-term fading wireless networks," *EURASIP Journal on Advances in Signal Processing*, vol. 2006, pp. 1–13, 2006.

[31] T. Wang, X. Wang, Y. Shi, W. Xin, Z. Jiang, T. Gao, and J. Duan, "Euler-maruyama method based channel prediction: An lde-net implementation and field evaluation," *IEEE Transactions on Vehicular Technology*, 2024.

[32] D. P. Kroese, T. Taimre, and Z. Botev, *Handbook of Monte Carlo methods*. N.J: Wiley, 2011.

[33] F. Han, Z. Wang, H. Dong, X. Yi, and F. E. Alsaadi, "Recursive distributed filtering for time-varying systems over sensor network via rayleigh fading channels: Tackling binary measurements," *IEEE Transactions on Signal and Information Processing over Networks*, vol. 9, pp. 110–122, 2023.

[34] S. Chai and V. K. Lau, "Multi-uav trajectory and power optimization for cached uav wireless networks with energy and content recharging-demand driven deep learning approach," *IEEE Journal on Selected Areas in Communications*, vol. 39, no. 10, pp. 3208–3224, 2021.

[35] X. Lv, Y. Li, Y. Wu, and H. Liang, "Kalman filter based recursive estimation of slowly fading sparse channel in impulsive noise environment for ofdm systems," *IEEE Transactions on Vehicular Technology*, vol. 69, no. 3, pp. 2828–2835, 2020.

[36] P. Singh, S. Srivastava, A. Mishra, A. K. Jagannatham, and L. Hanzo, "Sparse bayesian learning aided estimation of doubly-selective mimo channels for filter bank multicarrier systems," *IEEE Transactions on Communications*, vol. 70, no. 6, pp. 4236–4249, 2022.

[37] J. Yin, G. Zhu, X. Han, L. Guo, L. Li, and W. Ge, "Temporal correlation and message-passing-based sparse bayesian learning channel estimation for underwater acoustic communications," *IEEE Journal of Oceanic Engineering*, 2024.

[38] B. Zhu, Z. Zeng, J. Cheng, and N. C. Beaulieu, "On the distribution function of the generalized beckmann random variable and its applications in communications," *IEEE Transactions on Communications*, vol. 66, no. 5, pp. 2235–2250, 2017.

[39] J. M. Romero-Jerez and F. J. Lopez-Martinez, "A new framework for the performance analysis of wireless communications under hoyt (nakagami-q) fading," *IEEE Transactions on Information Theory*, vol. 63, no. 3, pp. 1693–1702, 2017.

[40] P. E. Kloeden, E. Platen, P. E. Kloeden, and E. Platen, *Stochastic differential equations*. Springer, 1992.

[41] N. B. Rached, A. Kammoun, M.-S. Alouini, and R. Tempone, "Unified importance sampling schemes for efficient simulation of outage capacity over generalized fading channels," *IEEE Journal of Selected Topics in Signal Processing*, vol. 10, no. 2, pp. 376–388, 2015.

[42] N. Ben Rached, A.-L. Haji-Ali, G. Rubino, and R. Tempone, "Efficient importance sampling for large sums of independent and identically distributed random variables," *Statistics and Computing*, vol. 31, no. 6, p. 79, 2021.

[43] E. Ben Amar, N. Ben Rached, A.-L. Haji-Ali, and R. Tempone, "State-dependent importance sampling for estimating expectations of functionals of sums of independent random variables," *Statistics and Computing*, vol. 33, no. 2, p. 40, 2023.

[44] N. Nüsken and L. Richter, "Solving high-dimensional hamilton–jacobi–bellman pdes using neural networks: perspectives from the theory of controlled diffusions and measures on path space," *Partial differential equations and applications*, vol. 2, pp. 1–48, 2021.

[45] N. B. Rached, A.-L. Haji-Ali, S. M. S. Pillai, and R. Tempone, "Single level importance sampling for mckean-vlasov stochastic differential equation," *arXiv preprint arXiv:2207.06926*, 2022.

[46] B. Øksendal and B. Øksendal, *Stochastic differential equations*. Springer, 2003.

[47] D. Revuz and M. Yor, *Continuous martingales and Brownian motion*. Springer Science & Business Media, 2013, vol. 293.

[48] D. Revuz, M. Yor, D. Revuz, and M. Yor, "Representation of martingales," *Continuous Martingales and Brownian Motion*, pp. 168–205, 1991.

[49] I. Gyöngy, "Mimicking the one-dimensional marginal distributions of processes having an itô differential," *Probability theory and related fields*, vol. 71, no. 4, pp. 501–516, 1986.